EUKARYOTIC CELL, Jan. 2006, p. 26–44 Vol. 5, No. 1
1535-9778/06/$08.00+0 doi:10.1128/EC.5.1.26–44.2006

Genome-Based Approaches to Understanding Phosphorus Deprivation Responses and PSR1 Control in *Chlamydomonas reinhardtii*†‡

Jeffrey L. Moseley,[1]* Chiung-Wen Chang,[2] and Arthur R. Grossman[1]

Carnegie Institution, Department of Plant Biology, 260 Panama Street, Stanford, California 94305,[1] and Department of Statistics, Sequoia Hall, 390 Serra Mall, Stanford University, Stanford, California 94305-4065[2]

Received 4 August 2005/Accepted 31 October 2005

The *Chlamydomonas reinhardtii* transcription factor PSR1 is required for the control of activities involved in scavenging phosphate from the environment during periods of phosphorus limitation. Increased scavenging activity reflects the development of high-affinity phosphate transport and the expression of extracellular phosphatases that can cleave phosphate from organic compounds in the environment. A comparison of gene expression patterns using microarray analyses and quantitative PCRs with wild-type and *psr1* mutant cells deprived of phosphorus has revealed that PSR1 also controls genes encoding proteins with potential "electron valve" functions—these proteins can serve as alternative electron acceptors that help prevent photodamage caused by overexcitation of the photosynthetic electron transport system. In accordance with this finding, phosphorus-starved *psr1* mutants die when subjected to elevated light intensities; at these intensities, the wild-type cells still exhibit rapid growth. Acclimation to phosphorus deprivation also involves a reduction in the levels of transcripts encoding proteins involved in photosynthesis and both cytoplasmic and chloroplast translation as well as an increase in the levels of transcripts encoding stress-associated chaperones and proteases. Surprisingly, phosphorus-deficient *psr1* cells (but not wild-type cells) also display expression patterns associated with specific responses to sulfur deprivation, suggesting a hitherto unsuspected link between the signal transduction pathways involved in controlling phosphorus and sulfur starvation responses. Together, these results demonstrate that PSR1 is critical for the survival of cells under conditions of suboptimal phosphorus availability and that it plays a key role in controlling both scavenging responses and the ability of the cell to manage excess absorbed excitation energy.

While phosphorus (P) is an abundant element in the Earth's crust, its availability can limit the growth of organisms present in both aquatic and terrestrial environments. P is essential for many fundamental processes that sustain life, including nucleic acid synthesis, membrane synthesis, energy metabolism, signaling, redox reactions, and modification of protein activities. The major form of P readily assimilated and utilized by most organisms is the phosphate anion (P_i). While available P_i (soluble P_i) is generally present at concentrations of <10 μM, most organisms require cellular P_i concentrations in the millimolar range (for reviews, see references 4, 40, and 45). For this reason, P_i supplementation is necessary to boost crop production and is included as a major constituent of fertilizers. However, following the introduction of P_i into soils, it can be rapidly precipitated as insoluble salts, become adsorbed to soil particles, or leach from agricultural fields, contaminating both groundwater and aquatic ecosystems. Manipulation of crop species to improve their ability to mobilize soil P_i may result in increased agricultural yields and a slowing of the consumption of exhaustible P_i sources.

Eukaryotic signal transduction pathways for sensing and responding to P starvation have been best studied in the yeast *Saccharomyces cerevisiae*. P-deficient *S. cerevisiae* cells increase their capacity for P_i uptake by expressing a high-affinity P_i transport system, mainly the Pho84p H^+/P_i symporter, which operates at acidic pHs (3, 6). The Pho89p protein is a Na^+/P_i cotransporter and may be utilized at more alkaline pHs (29). P_i that is covalently bound to organic molecules may be mobilized by cleavage by an acid phosphatase encoded by the *PHO5* gene (reviewed by Vogel and Hinnen [50] and by Oshima [36]). There are many genes that are coregulated under P starvation conditions in *S. cerevisiae*, forming the PHO regulon (35). Changes in gene expression that accompany P starvation of *S. cerevisiae* are regulated by a system comprised of a cyclin (Pho80) and a cyclin-dependent kinase (Pho85). Under P-replete conditions, the kinase activity of Pho80/Pho85 catalyzes hyperphosphorylation of the Pho4 transcription factor, which is then excluded from the nucleus. When P becomes limiting, the cyclin-dependent kinase inhibitor Pho81 is activated, preventing Pho80/Pho85 kinase activity and leading to hypophosphorylation of Pho4 and its subsequent import into the nucleus. Once in the nucleus, Pho4 and Pho2 interact, populating the promoters of target genes and activating gene expression (reviewed by Lenburg and O'Shea [26]).

In photosynthetic eukaryotes, P_i is also critical for chloroplast function. P_i must be transported from the cytoplasm of the cell, across the double membrane of the plastid envelope, and into the chloroplast stroma, where it is used to satisfy the biosynthetic and energetic requirements of the organelle. P_i is needed for both DNA and RNA synthesis within the chloroplast, as the plastids contain their own genomes and ribosomes, and each chloroplast usually has multiple chromosome copies.

* Corresponding author. Mailing address: Carnegie Institution, Department of Plant Biology, 260 Panama Street, Stanford, CA 94305. Phone: (650) 325-1521, ext. 238. Fax: (650) 325-6857. E-mail: Jeffrey.Moseley@stanford.edu.

† Supplemental material for this article may be found at http://ec.asm.org/.

‡ This is Carnegie Institution publication no. 1725.

Photosynthetic generation of ATP and the synthesis of phospholipids represent other critical chloroplast activities requiring P_i, and the phosphorylation of polypeptides of the photosynthetic apparatus modulates the properties of light-harvesting functions in response to changing environmental conditions (55). Furthermore, P limitation leads to depletion of the pool of phosphorylated intermediates in the pentose-phosphate cycle, which results in a marked reduction in photosynthetic carbon fixation (5, 22). Studies with *Chlamydomonas reinhardtii* have demonstrated that P and sulfur deprivation causes a similar loss of photosynthetic electron transport activity, the consequence of a combination of reduced photosystem II (PS II) abundance, accumulation of PS II Q_B nonreducing centers, an increase in nonphotochemical quenching, and an increase in the tendency of the cells to be in state II (53). These processes all redirect absorbed excitation energy away from PS II and linear electron transport. The observations described above support the idea that when nutrient availability limits the growth of the cell, a suite of mechanisms are mobilized to manage/dissipate excess absorbed light energy, reducing the potential of the system to generate reactive oxygen species which could cause severe cellular damage.

Little is known about the regulatory pathways by which plants and algae sense and respond to P deficiency. Genetic screens for *C. reinhardtii* mutants with a diminished P_i uptake capacity or reduced alkaline phosphatase activity during P-limited growth (46, 54) led to the discovery of the *p*hosphorus *s*tarvation *r*esponse 1 (*PSR1*) gene, which encodes a nucleus-localized factor with a MYB-like DNA binding domain and a coiled-coil protein-protein interaction domain (54). *PSR1* is required for normal growth and the synthesis of alkaline phosphatase following starvation of the cells for P. Furthermore, the abundance of the *PSR1* transcript and its protein product also increases during P starvation (54). Subsequent studies with *Arabidopsis thaliana* revealed that an analogous gene, *ph*osphate starvation *r*esponse 1 (*PHR1*), functions to elicit changes in root growth and morphology, anthocyanin production, and the activities of several P deficiency-inducible genes. These results suggest that the key regulators of the P deprivation responses in plants and *C. reinhardtii* (and perhaps other algae) are very similar, suggesting the possibility of common downstream signaling factors (42). However, it is not known whether *PSR1* and *PHR1* have dual functions, acting as both the sensor of intracellular P_i levels and the transcription factor that elicits altered gene expression. Recent findings have implicated an *Arabidopsis* SUMO E3 ligase, SIZ1, in the regulation of PHR1 activity (31), suggesting a multilevel control of plant responses to P_i deficiency.

In this study, we combine genome-based, molecular, and physiological approaches to examine P starvation responses in a wild-type *C. reinhardtii* strain and its isogenic *psr1* mutant. Potential P deprivation-responsive genes were identified by an examination of genomic information and by cDNA-based microarray analyses. A number of new P deficiency-responsive target genes were identified, many encoding proteins that would enable the cells to better cope with excess absorbed excitation energy, limiting the extent of potential photodamage during P deprivation; these stress-related genes may be directly under PSR1 control. The importance of these genes was suggested by experiments in which elevated light levels caused a dramatic loss of viability of *psr1* mutant, but not wild-type, cells during P deprivation.

MATERIALS AND METHODS

Strains and growth conditions. *Chlamydomonas reinhardtii* wild-type strain CC-125, a *psr1-1* mutant strain that was backcrossed five times to CC-125 (54), and pKS1-31, a *psr1-1* mutant strain complemented with the pKS1 plasmid containing a *PSR1* genomic clone (54), were used in the experiments. For RNA preparations, cultures were grown to mid-logarithmic phase in Tris-acetate-phosphate (TAP) medium on a rotary shaker (~150 rpm) at 25°C, with continuous illumination (~40 μmol photons m^{-2} s^{-1}). P-free Tris-acetate (TA) medium was prepared by substituting 1.5 mM potassium chloride for potassium phosphate, as described by Quisel et al. (39). To starve cells for P, cells were initially grown in TAP medium, harvested by centrifugation (4,000 × *g*, 5 min), washed twice with TA medium, and resuspended to a final cell density of 1×10^6 cell/ml in TA medium. P-starved cultures were maintained under the same growth conditions as the unstarved cells, except that all cultures were sampled 4, 12, 24, and 48 h after the initiation of P deprivation. For RNA preparation, cells were harvested by centrifugation in a model HN-SII clinical centrifuge (International Equipment Co.) at three-fourths the maximum speed (~5,800 rpm) for 10 min, and cell pellets were immediately frozen in liquid N_2 and stored at −80°C. Strains for high-light-intensity experiments were grown in liquid and solid TA and TAP media and in TA medium supplemented with 10 μM glucose-1-phosphate (Sigma Chemical Co., St. Louis, MO) at 27°C, with continuous illumination at 600 to 800 μmol photons m^{-2} s^{-1}.

RNA preparation. Cell pellets were maintained in liquid N_2. Each pellet was simultaneously thawed and homogenized in 8 ml of homemade Trizol reagent (Invitrogen Co., Carlsbad, CA) by continuously vortexing the suspension; the homogeneous suspension was then incubated at room temperature for at least 10 min. Chloroform (1.6 ml) was added to the suspension, and the tubes were shaken vigorously for 1 min and incubated at room temperature for an additional 2 to 3 min. Phase separation was achieved by centrifugation at 12,000 × *g* for 15 min, and 0.5 volume (3 to 4 ml) of 0.8 M sodium citrate–1.2 M NaCl was added to the aqueous phase, followed by the addition of 0.5 volume (compared to the initial volume) of isopropanol to precipitate nucleic acids. Precipitations were done at room temperature for 10 min, and the nucleic acid precipitate was collected by centrifugation at 12,000 × *g* for 10 min. Nucleic acids were washed with 8 ml of 75% ethanol, dried, and dissolved in diethyl pyrocarbonate-treated, double-distilled water. Poly(A) RNA was prepared using a MicroPoly(A) Pure small-scale mRNA purification kit (Ambion, Austin, TX) and was quantified fluorimetrically using a RiboGreen RNA quantification kit (Molecular Probes, Eugene OR) and a Tecan SPECTRAFluor fluorimeter (Zurich, Switzerland).

Preparation of fluorescent microarray probes. The incorporation of Cy3-dUTP and Cy5-dUTP (Amersham Pharmacia Biotech, Piscataway, NJ) was performed as described by Zhang et al. (56), with the following modifications: (i) 200 to 500 ng of poly(A) RNA was used as the template for labeling reactions; (ii) the deoxynucleoside triphosphate mixture contained 1 mM dTTP and 2.5 mM (each) of dATP, dCTP, and dGTP; (iii) labeling reactions were incubated at 42°C for 30 min, 45°C for 20 min, and 50°C for 30 min; (iv) incorporation of the fluorescent dyes into cDNA was not examined; (v) the reference RNA was isolated from log-phase cells of wild-type strain CC-125 prior to P deprivation; and (vi) samples prepared from P-starved (4, 12, 24, and 48 h) CC-125 and P-replete (0 h) and P-starved (4, 12, 24, and 48 h) *psr1-1* cells were compared to the reference sample.

Preparation, hybridization, washing, and scanning of microarrays. The printing and storage of array slides (v1.1) were performed as described by Zhang et al. (56) for the "2.7 k array," except that 3,079 different cDNA probes were printed on each slide. Additional details about the array are given at http://nostoc.stanford.edu/jeff/lab/chlamyarray/index.html and in Table 1 and Table S1 in the supplemental material. Slides were hydrated by holding them above a 90°C water bath for ~3 s and were then immediately dried on a 100°C hot plate for ~5 s. DNAs were cross-linked by UV radiation at 300 mJ in a UV Stratalinker 1800 (Stratagene, La Jolla, CA). Prehybridization was performed by baking the slides at 65°C for 10 min, followed by a 30- to 60-min incubation at 50°C in prehybridization buffer containing 3× SSC (1× SSC is 0.15 M NaCl plus 0.015 M sodium citrate), 0.1% sodium dodecyl sulfate, and 0.1 mg/ml bovine serum albumin. Slides were washed with water and then isopropanol, each for 2 min at room temperature, and then dried by centrifugation for 5 min in a SpeedVac Plus, model SC210A (Savant, Holbrook, NY). Hybridization, washing, and scanning of the slides were performed as described by Zhang et al. (56), except that the hybridization solution was prepared by mixing 20 μl of hybridization buffer with 20 μl of the labeled probes, and the fluorescence images from 12 complete array sets (three slides per time point, with four copies of each cDNA per slide) were

TABLE 1. Transcripts showing ≥2.5-fold change in transcript abundance during phosphate deprivation

CloneID[a]	Annotation	Direction of change in transcript abundance[b]		Fold change in transcript abundance[c]								
				CC-125				*psr1* mutant				
		CC-125	*psr1*	4 h	12 h	24 h	48 h	0 h	4 h	12 h	24 h	48 h
	Photosynthesis/respiration/electron transport											
894087e11	Putative 1, 4-benzoquinone oxidoreductase (flavodoxin-like domain)	.+++	.....	2.43	2.70	2.76	2.77	0.80	1.36	1.20	0.79	0.81
894066e12	HYD2, Fe-hydrogenase 2	..++	.....	0.95	0.96	6.34	7.23	0.88	1.13	0.61	0.64	0.73
894098f02	TBD1, required for translation of chloroplast D2 protein	.+.+	.....	2.27	3.22	2.42	2.96	0.83	1.67	1.00	0.87	0.94
894069c09	PETF2, ferredoxin	..+.	.....	0.58	0.88	2.53	1.22	1.23	0.43	0.94	0.79	0.95
894077c04	LhcSR3, stress-related chlorophyll a/b binding protein, 83% identity to LI818r-1	...+	.....	0.84	1.05	1.28	14.72	0.86	1.13	1.14	0.94	1.19
Stern:H01	HemA, glutamyl-tRNA reductase	...+	.....	1.91	1.22	1.57	3.87	0.67	0.99	1.08	1.28	1.40
894097e05	LI818r-2/LhcSR2	..+.	..+++	0.91	1.52	7.25	2.27	0.96	0.59	5.93	2.60	4.73
Stern:A04	PSAD	..+.	..+++	1.40	1.52	2.63	1.63	1.28	2.11	3.18	2.77	2.79
963045c07	CCP2, low-CO_2-inducible 36-kDa chloroplast envelope protein	...+	..+..	2.44	1.15	1.74	10.66	1.10	1.10	2.54	2.22	2.46
1031072g10	Similar to chloroplast SRP54	**.*	....+	NA	NA	6.13	NA	0.09	2.06	9.58	4.05	7.02
1031058c06	PSY, phytoene synthase thioredoxin, protein disulfide	...−	..+++	0.72	0.83	1.00	0.09	2.08	2.01	4.15	6.61	8.78
1031086a06	Isomerase	..−−	..+++	0.01	0.05	0.03	0.01	1.11	1.11	5.80	14.16	8.28
894033H06	LHCA3	...−	.....	1.11	0.77	1.00	0.36	0.75	0.92	0.55	0.42	0.40
894078C01	LHCA9	...−	.....	1.10	0.69	1.10	0.23	0.87	1.02	0.57	0.43	0.45
963069C06	LHCBM1	...−	.....	1.00	0.76	1.12	0.40	0.73	0.94	0.47	0.44	0.40
894017C09	PETF1	...−	.....	0.95	0.81	0.95	0.39	0.82	0.98	0.49	0.46	0.47
894089E08	PETN, cytochrome b6f complex; subunit PetN; chloroplast targeted	...−	.....	1.01	0.79	0.81	0.40	0.69	0.83	0.59	0.57	0.55
894002C07	PETO	...−	.....	0.82	0.65	0.53	0.12	0.86	0.95	0.43	0.60	0.58
894005B12	LIL polypeptide (LHC family)	.−−−	..−..	0.73	0.36	0.37	0.17	0.89	0.91	0.37	0.68	0.73
963046B11	PETF5	.−.−	−−−−−	1.05	0.35	0.46	0.34	0.25	0.15	0.14	0.14	0.13
894066E11	CHL27B (CRD1)	...−	.−−−−	0.84	0.49	0.61	0.18	0.47	0.33	0.27	0.28	0.28
963047H05	LHCA2	...−	..−−−	0.98	0.65	0.95	0.24	0.73	0.87	0.37	0.31	0.28
963042A01	LHCA5	...−	..−−−	1.14	0.56	1.05	0.21	0.74	0.80	0.34	0.40	0.34
894052A01	LHCB (CP26)	...−	..−−−	0.98	0.70	0.92	0.30	0.75	0.92	0.29	0.24	0.20
894069E01	PETE/PCY1	...−	...−−	0.96	0.88	1.07	0.37	0.87	0.89	0.50	0.38	0.34
894083B07	PSAE	...−	...−−	1.28	0.71	1.25	0.30	0.80	0.94	0.45	0.38	0.31
894086C09	PSAK	...−	....−	1.15	0.68	1.15	0.36	0.76	0.82	0.48	0.42	0.34
963046C03	Putative luminal polypeptide	...−	..−..	1.08	0.71	0.91	0.34	0.77	0.78	0.32	0.41	0.41
963042g07	GSA, glutamate-1-semialdehyde 2,1-aminomutase	...−	..−..	0.72	0.55	0.34	0.08	0.75	0.79	0.34	0.72	0.66
lhcbm8	LHCBM8	....	..−−−	1.25	0.80	1.35	0.44	0.72	0.76	0.29	0.17	0.16
963041E04	PSBQ (OEE3)	....	...−−	0.99	0.74	0.97	0.66	0.75	0.84	0.40	0.35	0.38
894100A05	PSAG	....	....−	1.13	0.83	1.20	0.45	0.65	0.77	0.53	0.41	0.37
	Pentose phosphate pathways/starch											
894008B02	GLPV, glycogen/starch phosphorylase	.+++	.....	1.07	3.57	5.77	6.28	0.68	1.28	1.38	1.16	1.44
894080B03	GAP1, glyceraldehyde-3-phosphate dehydrogenase	.+++	.....	1.01	4.06	5.61	5.74	0.83	1.06	1.20	0.71	0.66
894092f08	Alpha-amylase	..++	.....	0.91	0.63	4.07	5.52	0.43	1.19	0.42	0.86	1.19
894066h04	Similar to GP1 (glycogen phosphorylase 1)	..+.	.....	0.77	1.22	2.59	1.81	0.77	0.64	0.90	0.51	0.91
894038d10	PFP1, pyrophosphate-dependent phosphofructo-1-kinase	...+	.....	1.06	1.97	1.93	3.11	1.29	1.26	1.31	1.30	1.14
963048d01	STA2, granule-bound starch synthase I	..++	...++	1.70	1.76	3.15	3.98	0.96	1.20	2.03	2.83	2.67
894037H05	TAL1, transaldolase	...−	.....	1.11	0.62	0.41	0.32	1.07	1.17	0.72	0.69	0.82
894022G03	PCK (phosphoenolpyruvate carboxykinase)	...−	..−..	1.22	0.57	0.51	0.32	0.59	0.71	0.27	0.54	0.47
894040F03	PGK	....	..−..	1.16	0.82	1.50	0.75	0.97	0.88	0.39	0.59	0.55
	Ribosomal proteins (RP)											
894064a06	Probably Ribosomal_S7 ribosomal protein S7p/S5e	+.−.	..+++	15.50	0.15	0.04	0.09	1.25	0.81	11.54	22.84	22.53

894026G08	RPSCL1	..−−	.....	1.19	0.88	0.16	0.07	0.97	1.66	0.48	0.54	0.59
894044G05	RPSCL3	...−	.....	0.66	0.59	0.41	0.37	1.06	0.95	0.72	0.90	0.95
963032C10	RPLCL12	..−−	.....	0.69	0.48	0.24	0.28	1.00	0.73	0.72	1.04	1.03
894055G04	RPLCL18	..−.	.....	0.62	0.50	0.37	0.42	1.01	0.75	0.66	0.99	1.06
894027h10	Similar to Rps6, 30S ribosomal protein S6	..−−	.....	0.57	0.58	0.27	0.33	1.08	0.75	0.66	0.91	0.92
894014a03	RPSC17, 30S ribosomal protein S17 nucleus-encoded chloroplast protein	..−−	.....	0.60	0.52	0.29	0.35	1.37	0.97	0.72	1.08	1.02
894071g09	RPSc10, 30S ribosomal protein S10 nucleus-encoded chloroplast protein	..−−	.....	0.61	0.55	0.34	0.28	1.12	0.88	0.76	1.08	1.13
	Phosphate transport											
894044h02	PTB2, putative P_i transporter B2	.+++	.....	2.22	14.27	29.57	21.86	0.73	0.61	1.89	1.25	1.17
894099g11	PTB4, putative P_i transporter B4	..+.	.....	1.38	2.26	2.80	1.20	0.62	0.69	1.07	0.85	1.07
1024014a06	PTA3, putative P_i transporter A3	..++	.....	1.87	1.35	3.77	4.71	1.13	1.11	0.86	1.29	1.28
	Sulfur metabolism											
963027A09	SBDP1 (selenium binding protein)	..+.	..+++	0.99	1.38	2.87	1.43	1.04	1.23	3.19	5.49	5.19
894081F11	SAC1-like protein	....	..+++	0.25	0.56	0.48	0.51	0.76	1.72	5.60	5.77	5.32
1112050a12	Similar to ARS2 (25% identity)	....	..+++	0.57	0.44	1.72	0.23	0.93	1.23	5.94	20.25	17.49
894069d01	SIR1, sulfite reductase 1	....	..+++	0.61	0.36	0.29	0.18	1.49	0.74	3.84	4.27	2.97
1031097a10	Similar to CysW; sulfate transport system permease protein	...−	..+++	0.46	0.08	0.11	0.01	0.89	1.16	8.65	11.02	10.25
963024B05	OASTL4	....	....+	1.85	1.49	0.55	1.06	1.13	1.42	1.21	2.47	4.72
1031083g07	SAC1-like protein	−−.−	.....	0.01	0.01	0.11	0.01	0.35	0.40	0.57	0.92	0.94
	Other metabolic/biosynthetic processes											
894081C10	NNT, NAD transhydrogenase	.+++	.....	1.00	3.80	3.13	3.06	0.68	1.08	0.63	0.47	0.53
894049g01	Ca^{2+}/H^{+} antiporter VCX1	.+++	.....	1.09	2.00	3.08	5.40	0.94	0.85	1.15	1.03	1.04
894020c10	Similar to zinc-dependent alcohol dehydrogenase	..++	.....	1.69	0.97	2.53	3.58	1.57	1.57	1.35	1.57	1.57
894062A09	THIH, thiazole biosynthesis protein	..++	.....	2.04	1.10	2.57	5.06	0.86	0.96	0.50	0.45	0.47
894092h09	NAR1, 2, putative nitrite transporter	...+	.....	0.97	1.12	1.10	2.53	1.17	1.06	0.99	0.75	0.83
894038D07	PFL, pyruvate formate lyase	...+	.....	0.97	1.20	1.79	3.57	0.89	0.92	0.87	0.98	1.00
894078e01	UDP-glucose dehydrogenase	.+..	.....	1.47	3.98	0.78	1.94	1.09	1.35	1.49	0.80	1.32
963047a02	Ribonucleotide reductase large subunit	.+..	.....	0.69	2.54	0.65	0.63	1.60	1.84	1.41	0.85	0.74
963031a11	SEC61g, ER protein translocation SEC61 gamma subunit	.+..	.....	1.68	4.51	0.76	0.84	1.09	1.20	0.97	0.47	0.69
894068F05	dTDP-glucose 4-6-dehydratase	.+..	.....	1.24	3.88	0.89	0.98	0.83	1.19	1.19	0.72	1.00
963070H06	SDC1, serine decarboxylase	.+++	..++.	1.54	2.81	3.77	12.16	1.71	1.83	2.76	3.37	2.50
1112084g04	Peptide of methionine sulfoxide reductase	..+.	....+	0.40	0.29	20.49	0.11	1.07	50.00	3.64	0.54	9.11
963035c12	POLA4, similar to eukaryotic DNA polymerase alpha subunit 4 (primase)	.+.−	.+...	0.18	4.89	2.31	0.08	2.10	2.71	2.47	0.25	1.30
1031076e05	LIG1, putative ATP-dependent DNA ligase	....	..+++	0.29	0.90	1.56	0.86	2.43	1.68	19.26	33.15	25.09
894005h05	LEU1, putative isopropylmalate dehydratase; leucine biosynthesis	....	...++	0.53	0.59	0.39	0.69	1.24	0.93	2.43	3.01	3.27
894018d09	Beta-ketoacyl-CoA synthase	....	...++	2.06	1.59	0.94	1.30	1.41	0.90	1.77	2.78	2.89
894064A10	ILV3, dihydroxy-acid dehydratase	....	...+.	0.94	1.41	0.72	0.85	1.03	0.94	1.72	2.51	2.13
1031025a01	NADH-dependent glutamate synthase	−..−	..++.	0.01	0.04	0.34	0.01	1.30	1.10	3.29	3.63	2.20
1031069f10	Thioredoxin, protein disulfide isomerase	−−−−	...+.	0.01	0.01	0.01	0.01	0.28	2.28	3.88	6.62	0.48
1112094d03	MDHP, plastid malate dehydrogenase (NADP)	...−	....+	0.32	0.02	0.11	0.01	1.00	0.30	0.98	1.71	11.39
963047D02	SAS1, S-adenosylmethionine synthetase	...−	.....	1.10	1.23	0.46	0.18	0.88	0.89	0.81	0.42	0.43
894103C12	SAH1, S-adenosylhomocysteine hydrolase	...−	.....	1.13	1.54	0.44	0.10	1.26	0.99	1.20	0.54	0.69
963042H06	ACH, aconitate hydratase	...−	.....	1.30	0.84	0.56	0.29	0.71	0.71	0.50	0.54	0.43
963044D08	APOC, apospory-associated protein	...−	.....	0.90	1.13	0.65	0.26	0.67	0.71	0.61	0.43	0.45
894018e08	MDH2, malate dehydrogenase	...−	.....	1.12	0.97	0.89	0.38	0.87	0.84	0.75	0.67	0.66
1031043c06	URIC(UOX, UO), uricase, urate oxidase	...−	.....	0.98	1.07	1.18	0.28	1.10	1.01	0.67	0.47	0.71

Continued on following page

TABLE 1—*Continued*

CloneID[a]	Annotation	Direction of change in transcript abundance[b]		Fold change in transcript abundance[c]								
				CC-125				*psr1* mutant				
		CC-125	*psr1*	4 h	12 h	24 h	48 h	0 h	4 h	12 h	24 h	48 h
894042f02	APOC, apospory-associated protein	. . . −	. . . . .	1.16	0.84	0.83	0.40	0.88	0.74	0.77	0.65	0.69
963041f09	Argininosuccinate synthase	. . . −	. . . . .	1.10	1.12	0.96	0.38	1.02	0.94	0.99	0.90	0.73
963069c02	Ferredoxin-dependent glutamate synthase	. . . −	. . . . .	0.55	0.87	0.34	0.36	1.37	0.88	1.29	1.30	1.94
963028B11	SERA, putative D-3-phosphoglycerate dehydrogenase	. . − .	. . . . .	0.81	2.31	0.32	0.44	1.17	0.70	1.77	1.22	1.20
963041C09	THI4, putative thiamine biosynthesis protein	. . . −	. . . − .	1.07	1.54	0.87	0.37	1.28	1.42	0.45	0.31	0.43
963045H04	ACS3, putative acetyl-CoA synthetase	. . . −	. . − . .	1.26	0.47	0.54	0.03	1.00	1.07	0.37	0.49	0.49
963026e04	MAS, malate synthase, glyoxysomal	. . . −	. . − . .	0.94	0.43	0.47	0.04	0.78	0.84	0.34	0.60	0.64
	Transcription/translation/regulatory elements											
963045g03	Putative GPR/FUN34 family protein, similar to YaaH	. . ++	. . . . .	1.51	1.36	2.76	5.31	0.95	1.17	1.31	1.19	1.46
894096C06	Sensory opsin A	. . . +	. . . . .	1.02	0.89	1.65	2.80	0.60	0.75	0.65	0.72	0.72
963031f04	HKR2, putative histidine kinase response regulator; has PAC motif, histidine kinase, and response regulator receiver domains; probably no extracellular receptor domain	. . . +	. . . . .	2.37	0.61	1.00	2.53	1.08	1.24	1.36	0.98	0.99
963016f07	CDKG1, cyclin-dependent kinase	. . . +	. . . . .	1.09	1.90	1.66	3.14	1.37	1.78	1.60	1.02	1.21
894040c06	Similar to Mob1/phocein family cell cycle-associated protein	. . . +	. . . . .	1.51	0.94	1.87	3.56	1.30	1.41	1.26	1.45	1.26
963030e06	VTC1, vacuolar transport chaperone, similar to Nrf1, negative regulator of Cdc42p	. . . +	. . . . .	0.75	1.31	1.51	2.69	0.83	0.98	1.03	0.85	0.87
894071a05	MIND, cell division inhibitor	. + . .	. . . . .	0.98	3.07	1.07	0.75	1.95	1.92	1.81	0.85	0.95
894069A01	HMGB1, high-mobility-group DNA binding protein	. + . .	. . + . .	1.09	11.01	1.77	1.09	1.78	2.42	2.96	0.86	1.00
894040c05	CKS1, cyclin-dependent kinase regulatory domain-containing protein	. . . .	. . + . +	2.83	2.76	0.89	2.14	2.00	0.49	3.62	1.63	3.27
1031086f11	RPT5, 26S proteasome regulatory complex, base subcomplex, ATPase RPT4 (subunit 6A)	. − . −	. . +++	1.65	0.10	1.35	0.01	2.18	0.24	17.22	19.97	21.65
1031106c01	IF2G, putative eukaryotic translation initiation factor eIF2 gamma	. − . −	. . . + .	0.01	0.01	0.14	0.01	0.28	2.51	4.58	5.20	2.60
894001e02	IF3B, putative eukaryotic translation initiation factor 3 subunit	. . −−	. . . . .	0.74	0.62	0.14	0.09	1.30	0.99	0.87	0.72	1.08
894017c04	COP1, opsonin-related, retinal binding protein; chlamyopsin	. . . −	. . . . .	0.56	0.65	0.47	0.39	0.97	0.92	0.57	0.65	0.70
963043e10	IPY3, inorganic pyrophosphatase/nucleosome remodeling factor	. . −−	. . −−−	1.16	0.90	0.32	0.22	0.83	0.70	0.37	0.35	0.38
894006F01	SKS1-like protein kinase	. . . .	. . −−−	0.70	0.78	0.59	0.41	0.64	0.72	0.31	0.26	0.33
	Proteolysis/stress-related proteins											
894060g11	DHAR, GSH-dependent dehydroascorbate reductase	. . ++	. . . . .	1.24	0.92	3.25	10.42	0.92	1.15	1.61	1.73	1.42
894008C03	PTOX1, quinol-to-oxygen oxidoreductase	. . . +	. . . . .	0.29	1.72	2.25	13.53	1.12	0.87	1.34	1.29	1.39
894022h10	Putative glutathione S-transferase	. . . +	. . . . .	0.99	2.28	1.77	3.25	1.01	1.32	2.03	1.94	1.98
894099a12	Similar to prostaglandin D synthase GMP1, GDP-D-mannose pyrophosphorylase (D-mannose-1-phosphate guanylyltransferase)	. + . .	. . . . .	1.26	4.30	1.72	0.85	1.09	1.43	0.98	0.64	0.51
894044F09	AOX1, alternative oxidase 1	. . ++	. + . . .	2.10	1.52	6.98	8.74	0.86	3.98	1.08	1.88	1.40
963068F01	HS2C, putative chloroplast 22-kDa heat shock protein	. . . +	. . +++	1.44	0.86	1.15	8.04	0.96	0.77	5.80	6.96	6.92
894096A07	Putative chloroplast heat shock 22-kDa-like protein	. . . +	. . +++	1.31	0.93	0.89	6.46	1.35	1.92	4.17	5.23	6.19
894082a11	Putative glutathione S-transferase	. . . +	. . +++	0.40	0.57	2.59	16.14	1.57	2.35	5.83	22.20	28.56
894008E11	SKP1 E3 ubiquitin ligase; similar to Skp1	. + . .	. . +++	1.63	2.88	1.21	1.91	1.19	1.43	3.08	2.62	2.79

963033H10	DEGP-like, serine endoprotease	...+	...++	1.08	1.17	1.16	2.57	1.04	0.94	2.30	2.59	2.71
894024A08	Aspartic proteinase, delta subunit	...+	....+	0.66	1.07	1.62	9.61	1.31	0.86	1.62	2.42	3.16
1031080d10	Similar to DnaJ, heat shock protein/overlaps with NTF-2 nuclear transport factor	....	..+++	0.75	0.44	1.24	0.08	2.18	1.57	10.57	18.74	17.45
1031078d05	Similar to homogentisic acid geranylgeranyl transferase	....	..+++	1.13	0.18	0.74	0.25	1.83	1.27	28.91	21.48	42.38
1031092c06	Probable aldo/keto reductase (related to aryl-alcohol dehydrogenases)	....	..+..	0.07	0.67	1.02	0.25	0.83	1.01	2.58	2.39	2.14
1031072e09	Subtilase serine protease	.−.−	..+++	0.01	0.01	0.26	0.01	0.35	3.92	33.94	16.46	48.13
1112094c03	Subtilase serine protease	−−.−	...++	0.01	0.01	1.10	0.01	3.48	0.41	5.40	4.54	7.79
1031045e11	DEGPc (HtrA), similar to DegP protease	.−.−	....	0.49	0.24	0.76	0.03	2.16	0.69	0.89	1.06	1.22
1031054d01	Similar to glutathione peroxidase	...−	.....	0.84	0.22	2.08	0.09	1.80	1.61	0.51	0.48	0.64
	Putative structural, surface, and matrix proteins											
963046E08	TUA1, a tubulin 1	.+.+	.....	1.76	2.94	1.47	1.60	1.05	1.75	1.54	1.07	1.00
963077B03	FMG1b, flagellar membrane glycoprotein 1b	.+.+	.....	2.05	2.54	2.09	2.52	0.80	1.53	1.05	0.90	0.84
894093H02	TUB2, b tubulin GI	++..	.....	3.05	4.44	1.50	1.01	1.21	2.20	1.46	0.89	0.86
894083H05	SYP71, syntaxin	...+	.....	2.23	2.55	0.70	4.74	1.76	1.65	1.47	1.62	1.37
894017B12	VFL2, centrin (caltractin)	.+..	.....	1.22	4.94	1.10	1.22	1.26	1.90	2.01	0.78	0.97
894056C11	TUB1, b tubulin 1	.+..	.....	2.26	3.67	1.76	1.77	1.00	2.27	1.49	1.27	1.24
963089h02	Gliding motility-related CaM kinase	.+..	.....	1.43	2.54	1.62	1.77	0.87	0.85	0.88	0.83	0.82
894006H07	CHLRE_650068, microtubule-associated protein	...+	..+++	1.40	0.53	1.06	9.83	1.00	2.75	8.07	10.36	8.22
963079b11	Similar to syntaxin 6	...+	..+..	3.26	0.49	1.45	3.41	0.36	0.38	2.53	1.18	2.07
1031108a08	KAT1, microtubule-severing protein katanin, p60 (catalytic) subunit	−−..	..+++	0.01	0.01	0.16	0.33	0.48	0.57	8.04	5.77	5.11
963046H09	HRP1, putative sulfated surface glycoprotein	....	....−	0.71	0.75	0.86	0.52	0.68	0.50	0.51	0.44	0.28
	ATPases/uncoupling proteins/transporters											
894071E08	Similar to mitochondrial substrate carrier	...−	.....	0.99	0.68	0.50	0.27	0.99	1.12	0.52	0.64	0.66
963089h03	ATPG, CFO ATP synthase subunit II precursor	...−	.....	0.90	0.66	0.59	0.28	0.80	0.79	0.69	0.60	0.52
894077b08	Similar to 2-oxoglutarate/malate translocator	...−	.....	1.22	0.81	0.85	0.21	0.61	0.78	0.46	0.45	0.50
894041h06	ATPC, ATP synthase gamma chain, chloroplast precursor	...−	.....	1.07	0.78	0.81	0.27	0.74	0.69	0.63	0.61	0.61
	Unknown											
894044C07	Unknown, similar to alcohol dehydrogenase/acetaldehyde dehydrogenase	++++	.....	2.65	3.80	5.80	7.37	0.81	1.01	1.34	1.45	1.61
894095h09	Unknown	.+++	.....	2.58	3.87	14.19	16.78	0.80	1.04	1.19	1.37	0.93
894054A11	Unknown	..++	.....	1.00	1.84	2.54	3.92	1.49	1.22	1.13	1.11	1.07
894056c02	Unknown, no gene model	..++	.....	0.80	1.36	3.06	4.24	0.84	1.11	1.02	0.84	0.73
963033D03	Unknown	...+	..+++	1.89	3.20	0.76	4.92	1.08	1.82	9.29	8.43	6.21
963032A08	Unknown	...+	..+++	1.41	1.96	1.78	5.44	0.43	1.49	9.45	16.45	14.13
894044E09	Unknown	...+	...++	1.25	1.13	0.95	5.15	0.96	1.07	2.41	2.86	2.66
963044B12	Unknown	...+	...++	0.91	1.04	1.31	3.05	0.90	1.21	1.97	2.56	3.90
894091E12	Unknown	...+	.−−−−	0.61	0.80	2.35	3.60	0.55	0.40	0.11	0.11	0.10
1031110h04	Unknown	....	.++++	0.13	0.93	0.94	1.64	1.15	3.21	22.83	25.69	29.43
894001H07	Unknown, putative protein in PetA-PetD intergenic region	....	..+++	0.56	0.25	1.11	0.01	0.37	1.59	50.32	56.85	122.9
963096E10	Unknown	....	..+++	1.65	0.79	0.78	0.72	0.82	0.37	2.76	3.07	3.95
963063B08	Unknown	....	..+++	1.07	0.78	0.76	1.07	0.75	1.00	3.29	3.90	4.51
963032A01	Unknown proline-rich protein	....	..+++	1.40	2.13	0.59	3.37	0.51	0.50	13.94	47.58	41.66
1031079a07	Unknown, THiJ/PfpI family protein	....	..+++	2.52	0.01	0.10	0.01	1.94	0.33	23.33	17.85	14.29
1112049b04	Unknown	....	..+++	0.16	0.14	0.52	0.29	1.67	1.03	9.39	16.74	29.73
1112051d02	Unknown, FAD-linked oxidase, 4Fe-4S ferredoxin	....	..+++	0.35	0.16	1.04	0.50	1.59	1.44	4.33	6.61	10.13

Continued on following page

TABLE 1—*Continued*

CloneID[a]	Annotation	Direction of change in transcript abundance[b]		Fold change in transcript abundance[c]								
				CC-125				*psr1* mutant				
		CC-125	*psr1*	4 h	12 h	24 h	48 h	0 h	4 h	12 h	24 h	48 h
894074e08	Unknown, GPR1/FUN34/yaaH family	. . — —	. . . . .	1.09	0.71	0.35	0.09	0.97	1.08	0.44	0.44	0.43
894029F01	Unknown	. . . .	. . — — —	0.46	0.80	0.87	1.87	0.70	0.56	0.08	0.06	0.03
894049E03	Unknown	. . . .	. . — — —	1.04	0.72	1.15	0.44	0.66	0.74	0.37	0.33	0.30
894083b06	Unknown	. . . .	. . — — —	1.15	0.84	1.09	0.42	0.57	0.71	0.35	0.21	0.18

[a] Identification number of the sequence read (EST) used to make the array element.
[b] Change in transcript abundance (+ or −) at the points 4, 12, 24, and 48 h after P depletion for CC-125 cells and 0, 4, 12, 24, and 48 h after P depletion of *psr1* cells relative to that of CC-125 at time 0. Ratios that do not meet the cutoff of 2.5-fold change or do not pass Student's *t* test for significance are represented by dots.
[c] NA, not enough high-quality data for statistical tests.

analyzed. Two independent sets of RNA samples were used for array analyses; a dye swap was performed using one of the RNA samples.

Analyses of microarray data. Images from scanned slides were imported into the Genepix Pro 3.0 program (Axon Instruments, Union City, CA), where the spot positions were defined and their intensities determined. Spot signals that were distorted by dust, high local background, or printing flaws or signals with high proportions of saturated pixels were not included in subsequent analyses. The data were imported into Genespring 6.1 software (Silicon Genetics, Redwood City, CA) and normalized using the software's standard "per spot" and "per chip" intensity-dependent (Lowess) normalization (http://stat-www.berkeley.edu/users/terry/zarray/Html/normspie.html). Error models were computed based on replicates. Signal ratios were considered to meet threshold criteria if they passed Student's *t* test for significance with a *P* value of ≤0.05 and a multiple testing correction adjustment using the method of Benjamini and Hochberg (2).

Gene identification. To identify specific genes in the *C. reinhardtii* genome, either sequence information from GenBank for previously isolated and characterized genes or sequence information from cDNAs or genomic DNAs from other organisms (mainly *A. thaliana* and cyanobacteria) was used to perform BLAST alignments against *C. reinhardtii* genomic (http://genome.jgi-psf.org/chlre2) and expressed sequence tag (EST) database (http://www.biology.duke.edu/chlamy_genome/search.html) sequences. Candidate orthologous and paralogous predicted proteins were aligned with each other and evaluated using CLUSTALW (48); identity shading was performed using GeneDoc software (33).

Quantitative real-time PCR. Isolated total RNA was treated with RNase-free DNase I (Ambion Inc., Austin, TX) and then extracted with phenol-chloroform to isolate the RNA. Real-time quantitative PCRs (qPCR) for all genes except *PTOX1*, *PTOX2*, *GAP1*, and *DHAR* were performed by using 0.1 μg of DNase-treated total RNA and an iScript One-Step RT-PCR kit with SYBR green (Bio-Rad Laboratories, Hercules, CA). The amplifications were performed using either an iCycler IQ or Chromo4 real-time PCR thermocycler (Bio-Rad Laboratories, Hercules, CA), with the following cycling conditions: (i) 50°C for 30 min for cDNA synthesis, (ii) 95°C for 5 min to denature reverse transcriptase, and (iii) 40 to 42 cycles of 95°C for 15 or 30 s and 60°C for 30 s, with fluorescence detection after the 60°C annealing/extension step. Melting curve analysis was performed on all PCRs to ensure that single DNA species were amplified, and product sizes were verified by agarose gel electrophoresis. Discrete products were not obtained with the one-step system for the *PTOX1*, *PTOX2*, *GAP1*, and *DHAR* transcripts; consequently, two-step qPCR analysis was performed for these transcripts. For cDNA synthesis, 1 μg of DNase I-treated total RNA was reverse transcribed by using a Superscript II kit (Invitrogen, La Jolla, CA) as described by the manufacturer. qPCR was performed using either a DyNAmo Hot Start SYBR green qPCR kit (MJ Research Inc., Waltham, MA) or IQ SYBR green supermix (Bio-Rad Laboratories, Hercules, CA) and analyzed with the Mx3005P qPCR system (Stratagene, La Jolla, CA) or the Chromo4 system (Bio-Rad Laboratories, Hercules, CA). Cycling conditions included an initial incubation at 95°C for 10 min followed by 40 to 45 cycles of 94°C for 10 s, 55°C to 60°C for 15 s, and 72°C for 10 to 15 s. The relative expression ratio of a target gene was calculated based on the $2^{-\Delta\Delta C_T}$ method (28), using the average cycle threshold (C_T) calculated from duplicate measurements. Relative expression ratios from two independent experiments are reported. The *CBLP* gene was used as a control gene, and each primer was designed by Primer3 software to distinguish the different isozymes.

Primers for real-time PCR were as follows: *CBLP*, forward (5′-CTTCTCGCCCATGACCAC-3′), reverse (5′-CCCACCAGGTTGTTCTTCAG-3′); *PHOX*, forward (5′-TTCCGTTTCCGTTCTCTGAC-3′), reverse (5′-CCCTGCATCTTGTTCTCCAG-3′); *PTB1*, forward (5′-GCTTCTGCATCGAGCTGTC-3′), reverse (5′-TTCCCTCCATCAGACCAATG-3′); *PBT2*, forward (5′-TGTGCTCGTGCATTCTCTTC-3′), reverse (5′-CCCTTGGTGAACACGAAGTAA-3′); *PTB3*, forward (5′-GCGAGAACTCCTACGTCCTG-3′), reverse (5′-AGTCCAGTCGCTGTTGGAAG-3′); *PTB4*, forward (5′-CCAACCTGGCAATCTACATG-3′), reverse (5′-GCCTTGTTCGAGTCCCAGT-3′); *PTB5*, forward (5′-CTCAACCCAGTTGGCAATTTACTTT-3′), reverse (5′-GCCTTGTTCGAGTCCCAGT-3′); *PTB6*, forward (5′-TTCTTCCTGAACCGCATCTT-3′), reverse (5′-GCTCTTCGCTCCCTTGTAGA-3′); *AOX1*, forward (5′-TGGGCTCCATAGCTTCGGTTC-3′), reverse (5′-GTGGCAGCGGGCTTGTGG-3′); *AOX2*, forward (5′-AGCATGTCAGGGCTTGTGT-3′), reverse (5′-GGCATCCTTGACATGACTCAG-3′); *PTOX1*, forward (5′-GACAGCCTGGACGCAGTG-3′), reverse (5′-GCAGTTGTTGATGAGCTTGC-3′); *PTOX2*, forward (5′-GGACAAGGCGTTGGAGAAC-3′), reverse (5′-CCGACACAGACAGCTCCAG-3′); *GAP1*, forward (5′-CTGGCGTGTTCACTGACATC-3′), reverse (5′-TTGACGCCCATCACATACAT-3′); *GAP2*, forward (5′-TTGAGTCTGTGGCGTACCTG-3′), reverse (5′-CCCTCAATGGACTTGCAGTT-3′); *GAP3*, forward (5′-CC

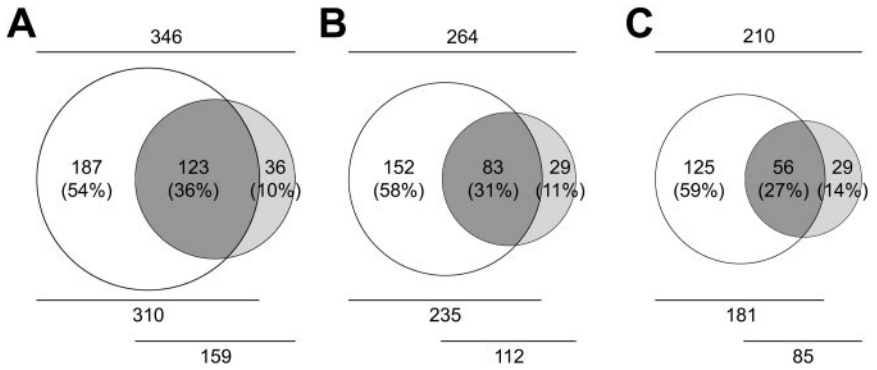

FIG. 1. Genes that exhibit altered transcript abundance during P deprivation. Proportional Venn diagrams representing genes in microarray experiments with altered transcript levels during P starvation are shown. The areas of the circles and of the overlapping regions are directly proportional to the numbers of genes represented. The total number of genes in both the wild type and the *psr1-1* strain that reached or surpassed the threshold ratio is shown above each overlapping diagram; the numbers below each diagram distinguish the genes altered in wild-type versus *psr1-1* cells. (A) Transcript levels altered by ≥2-fold; (B) transcript levels altered by ≥2.5-fold; (C) transcript levels altered by ≥3-fold.

GTGTCCTCCAAGTCTGG-3′), reverse (5′-CAGCAGCGCAGGAAGTTG-3′); *HYD1*, forward (5′-GCGACTGGTTCTGTGTGGAC-3′), reverse (5′-CAT TGGATTGTCCCACTCG-3′); *HYD2*, forward (5′-GCGAGTGGTTCTGTGT GAGC-3′), reverse (5′-CTGGTCCCAGTCACTGTCG-3′); *GPLV1*, forward (5′-GTGGACAGCGTCAACAACAT-3′), reverse (5′-ACTCCGCCTGGTCCT TGTAG-3′); *GPLV2*, forward (5′-ACTTCGGCTGGGAGGATTAC-3′), reverse (5′-CCACTCCGTCTGGTTCTTGT-3′); *DHAR*, forward (5′-GCCCAA GCTATACCATGCTG-3′), reverse (5′-TAGTCCACATGCTGCCACTC-3′).

Immunological detection of PHOX. *C. reinhardtii* cell cultures were concentrated by centrifugation and adjusted to a chlorophyll concentration of 1 mg/ml. The chlorophyll concentration was estimated according to the absorbance at 652 nm of 5-μl aliquots of cell suspension that were extracted in an 80% acetone–20% methanol mixture. Whole cell proteins equivalent to 10 μg of chlorophyll were solubilized in 1× Laemmli sample loading buffer, separated by discontinuous sodium dodecyl sulfate-polyacrylamide gel electrophoresis using a 7.5% polyacrylamide resolving gel, and transferred to polyvinylidene difluoride membranes (Pierce Biotechnology, Rockford, IL). Membranes were blocked for 1 h in a solution containing 5% dry milk and then incubated for at least 2 h with a 1/500 dilution of anti-PHOX antiserum (18) in 1% milk. A 1/3,000 dilution of alkaline phosphatase-conjugated goat anti-rabbit antiserum in 1% milk was used as the secondary antibody, and the alkaline phosphatase colorimetric reaction was performed as described by Sambrook et al. (44).

RESULTS

Microarray analyses. We used cDNA microarrays (56) to analyze the effects of P deficiency on transcript abundance in both a wild-type strain (CC-125) and a mutant (*psr1-1*) of *C. reinhardtii*; this mutant is abnormal in its responses to P deprivation (54). The relative levels of nearly 3,000 different transcripts of CC-125 were analyzed over a time course of P starvation. RNAs were isolated from cells 0, 4, 12, 24, and 48 h after they were transferred from nutrient-replete medium to medium devoid of P. Using cDNA-based arrays, the levels of transcripts at each of the time points were compared to those of CC-125 cells grown in nutrient-replete TAP medium (0 h). Transcript levels were filtered for significant elevation or diminution at one or more of the time points following the initiation of P starvation. The significance of the changes observed was tested using Student's *t* test. Venn diagrams were constructed to show the numbers of genes for which the levels of transcripts changed by ≥2-fold (Fig. 1A), ≥2.5-fold (Fig. 1B), and ≥3-fold (Fig. 1C), specifically in CC-125, in the *psr1-1* mutant, or in both strains. We chose to concentrate on those transcripts that exhibited a change of 2.5-fold or more following exposure of cells to P deprivation conditions. Table 1 shows the genes encoding the transcripts that changed by ≥2.5-fold in either wild-type cells or *psr1-1* cells; to be included in the table, this change had to be observed for at least one point during the time course of P deprivation, and it had to pass Student's *t* test for significance. The transcripts of 235 genes exhibited changes of ≥2.5-fold in wild-type cells during P deprivation, corresponding to somewhat less than 10% of the genes on the array. Of these, transcripts of 152 genes differentially accumulated in wild-type cells, but not in the *psr1-1* mutant; such genes are candidates for being directly regulated by PSR1. Furthermore, there were 29 transcripts in *psr1-1* cells, but not in wild-type cells, that changed in abundance during P deprivation. The genes encoding these transcripts most likely respond to secondary stress conditions that result from the inability of *psr1-1* cells to acclimate properly to P deficiency. An additional 83 transcripts differentially accumulated in both CC-125 and the *psr1-1* mutant during P deprivation, with the majority (53) being regulated in the same direction (either up or down) in the two strains, suggesting that PSR1 is not involved (or has minimal involvement) in the control of these genes. There was one transcript that increased by >2.5-fold in CC-125 and decreased in the *psr1-1* mutant; conversely, there were 30 transcripts that increased by 2.5-fold in the *psr1-1* mutant and decreased in the wild-type strain. These responses may also be primary or secondary responses to PSR1 production in the cell.

The genes in Table 1 are categorized according to the putative functions of their protein products, and within each category, those genes with similar patterns of transcript accumulation are grouped together. The subset of genes for which transcripts increase or decrease in wild-type cells, but not in the *psr1-1* strain during P starvation, may be controlled either directly or indirectly by PSR1. Among the genes in the category characterized by increased transcript abundance following P deprivation of wild-type cells are those encoding putative high-affinity P_i transporters, similar to Pho89 and Pho84 of *S. cerevisiae*; the *C. reinhardtii* genes encoding these transporters are designated *PTB2*, *PTB4*, and *PTA3*. The *PTB2* transcript level increased 20-fold or more during P deprivation. These P_i transporters may contribute to the high-affinity P_i uptake activity that has been associated with P-starved cells (24, 46).

A second set of six genes that may be under PSR1 control encode potential "electron valves," which are enzymes that may serve to protect the cell against oxidative damage resulting from overexcitation of the photosynthetic and respiratory electron transfer chains. Genes in this category encode AOX1, an isoform of a mitochondrial alternative oxidase, PTOX1, a terminal oxidase present in the plastid, and HYD2, an iron hydrogenase that can serve as an alternative electron acceptor for PS I. Interestingly, the transcripts for a plastid-targeted isoform of the glyceraldehyde-3-phosphate dehydrogenase (GAP; Calvin cycle enzyme) gene, *GAP1*, and for a starch phosphorylase gene, *GPLV*, also increase in a PSR1-dependent manner. Increasing carbon fixation coupled with the synthesis and storage of starch is another way that the cell can eliminate excess reductant generated by photosynthetic electron transport and diminish the probability of producing reactive oxygen species.

There are also 26 transcripts that increase in a PSR1-independent manner during P deprivation; the levels of these transcripts change to a similar extent in wild-type cells and the *psr1-1* mutant following the imposition of P deprivation. A number of genes encoding proteases and chaperones, listed under the heading "proteolysis/stress-related proteins" in Table 1, behave in this fashion. While we cannot formally rule out the possibility that genes which are regulated similarly in both the wild-type and *psr1* mutant strains may respond to the centrifugation and washing steps that precede the induction of P deprivation, in many cases elevated levels of the transcripts from these genes were observed at earlier time points following P starvation in the *psr1-1* mutant than in wild-type cells. Also, many of the responses were sustained over the 48-h time course of P deprivation. This suggests that these responses are neither induced by mechanical stress nor under PSR1 control but that the management of P resources (e.g., scavenging P from external and internal stores) in the mutant may be less effective than that in wild-type cells, which in turn can result in more rapid manifestation of PSR1-independent P deprivation responses. The levels of many transcripts encoding proteins required for photosynthesis also declined to similar extents in both strains. Overall, while a distinct subset of genes that respond to P deprivation conditions appears to be controlled by PSR1, a similar number of genes that are differentially expressed during P starvation are regulated by mechanisms that do not involve this transcription factor.

Genes potentially regulated by P availability based on genomic sequences. To analyze the expression of *C. reinhardtii* genes involved in the acquisition of P_i from the environment (specific responses), we surveyed the draft genome sequence for genes encoding potential secreted phosphatase enzymes and P_i transporters. A single gene encoding a potential phosphatase and multiple genes encoding potential P_i transporters were identified. Changes in the levels of the transcripts from these genes were examined using qPCR following exposure of cells to P starvation.

(i) PHOX, a calcium-dependent alkaline phosphatase. Using TBLASTN, we identified a gene on scaffold 86 of the *C. reinhardtii* version 3 genome sequence with strong similarity (E value = 0.0) to the PHOX alkaline phosphatase gene of *Volvox carteri* (18), as shown in the alignment in Fig. 2. PHOX is likely to be the abundant, inducible, extracellular alkaline phosphatase of *C. reinhardtii* that was characterized by Quisel et al. (39). This enzyme has a molecular mass of ~190 kDa, and its activity was demonstrated to be Ca^{2+} dependent and to peak in the basic pH range. The gene model on scaffold 86 (fgenesh1_pg.C_scaffold_86000013) has 57% identity with the *PHOX* gene of *V. carteri* (Fig. 2). A sequence gap on the genome scaffold coincides with a region close to the C-terminal end of the predicted *C. reinhardtii* protein that is missing in the alignment with *V. carteri* PHOX. Furthermore, no other significant matches to PHOX were identified in the genome. These results suggest that *C. reinhardtii* may have a single *PHOX* gene homolog and that this single gene is interrupted by a sequence gap in the draft genome sequence.

(ii) P_i transporter type B family (Pho89 homologs). At least eight potential homologs of the gene for the *Saccharomyces cerevisiae* Pho89 high-affinity Na^+/P_i symporter are present in the *C. reinhardtii* genome (Fig. 3). Two additional gene models with significant similarity to the *PTB* genes were not included in this analysis, as the sequences used for the gene model predictions were of poor quality. Interestingly, pairs of these genes (*PTB2* and *PTB3*, *PTB9* and *PTB12*, and *PTB4* and *PTB5*) are in close proximity and have the same 5′-to-3′ orientation in the genome, suggesting that they may have arisen from relatively recent gene duplications (Fig. 3A). The amino acid sequence identity is 96% between PTB2 and PTB3, 97% between PTB9 and PTB12, and 96% between PTB4 and PTB5. PTB6 is more closely related to PTB4, PTB5, PTB9, and PTB12 (69 to 71% identity) than to PTB2 and PTB3 (38% identity), and PTB1 is the most diverged member of the family, containing a large insertion of 1,107 amino acids and only exhibiting 34 to 43% identity to the other PTB polypeptides (when this insertion is excluded from the alignment) (Fig. 3B). This large, hydrophilic loop in PTB1 was described previously by Kobayashi et al. (24), who isolated the gene in a screen for arsenate-resistant *C. reinhardtii* mutants. The sequence identities of the *C. reinhardtii* PTB proteins to Pho89 from *S. cerevisiae* range from 19 to 23%, but the alignments show regions that are highly conserved between the yeast and algal proteins, especially at the N and C termini (data not shown).

(iii) P_i transporter type A family (Pho84 homologs). The *C. reinhardtii* genome contains genes for four potential homologs (PTA1 to PTA4) of the *S. cerevisiae* Pho84 high-affinity H^+/P_i cotransporter (Fig. 4). Three of the *PTA* genes are on the same scaffold (Fig. 4A), again suggesting that the expansion of this gene family is evolutionarily recent. The PTA3 and PTA4 proteins are the most similar, with 88% identity, but all of the PTA polypeptides are highly conserved, with a minimum of 73% sequence identity (Fig. 4B). Only 20 to 21% of the amino acids are conserved between the PTAs and Pho84, but a number of highly conserved motifs are located throughout the entire length of the sequences, with the exception of the very N- and C-terminal regions (data not shown).

Expression of *PHOX*, *PTB*, and *PTA* genes. qPCR analyses were performed to confirm the changes in transcript levels observed on the microarray and also to determine whether potentially P-regulated genes identified from the genomic sequence are controlled at the level of mRNA abundance. As previously noted, microarray analyses revealed increased *PTB2*, *PTB4*, and *PTA3* mRNA levels in wild-type cells, but not in the *psr1* mutant, during P starvation (Table 1). For *PTB2* and *PTB4*, peak increases in transcript abundance occurred at

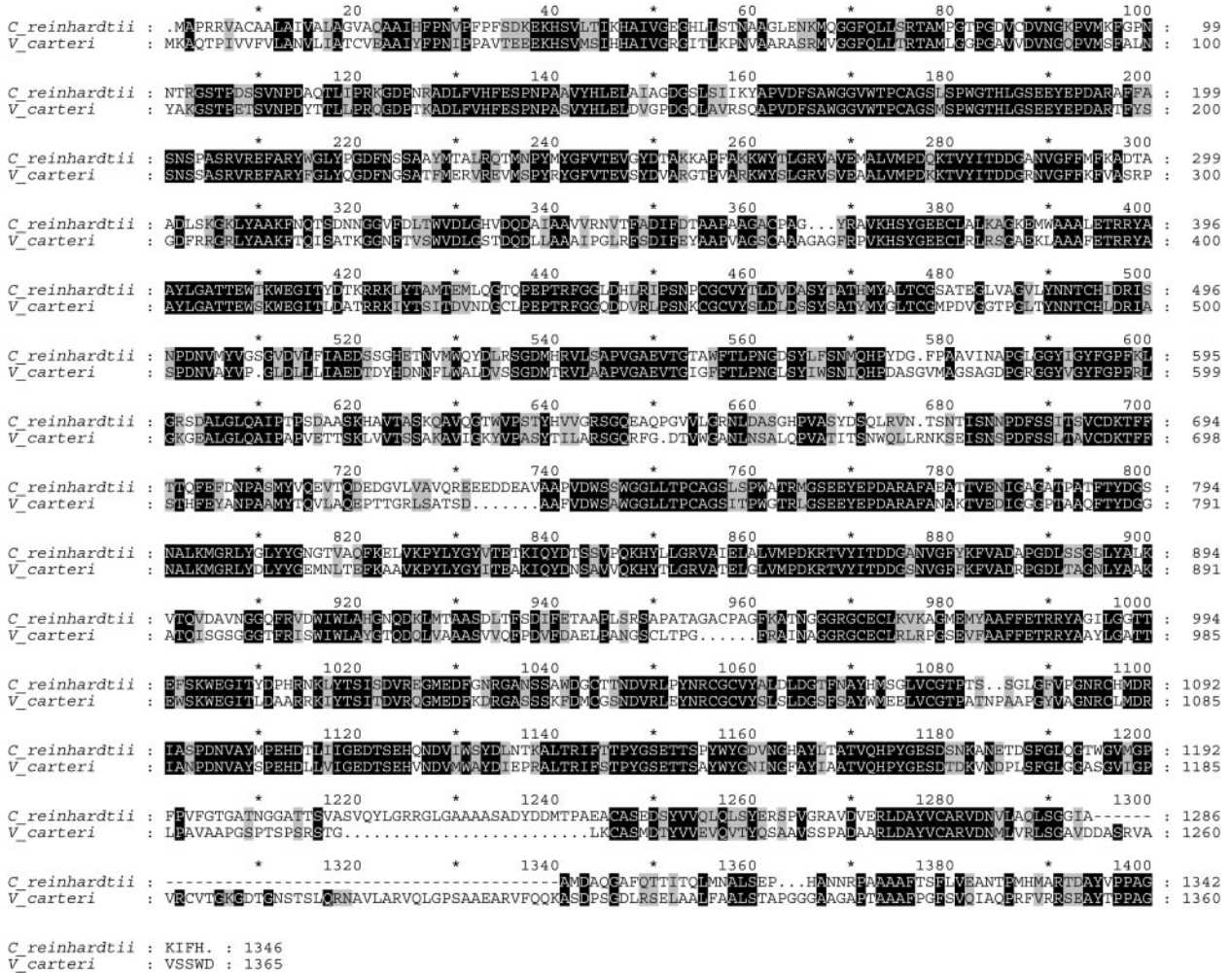

FIG. 2. Amino acid alignment of *V. carteri* and *C. reinhardtii* PHOX polypeptides. The diagram shows a CLUSTALW alignment of *V. carteri* PHOX (accession no. CAA10030) and the predicted polypeptide encoded by gene model fgenesh1_pg.C_scaffold_86000013, corresponding to the potential *PHOX* homolog deduced from the *C. reinhardtii* draft genome sequence. Black shading denotes sequence identity, and conservative amino acid changes are shaded gray. Gaps introduced by the alignment program are represented by dots, while dashes indicate a gap in the *C. reinhardtii* PHOX polypeptide sequence that is due to a missing nucleotide sequence on the genomic scaffold.

24 h following the transfer of cells to medium devoid of P, with a slight decline in the level after 48 h; therefore, we considered 24 h to be an appropriate starvation time to examine transcript abundance for other members of the P_i transporter gene families. The qPCR results for transcripts encoded by *PHOX* and the different *PTB* and *PTA* gene family members from both wild-type cells and the *psr1-1* mutant after 24 h of P starvation are presented relative to those for the same transcripts in wild-type cells or *psr1-1* mutant cells in the logarithmic phase of growth under P_i-replete conditions (0-h references).

As shown in Table 2, for wild-type cells (CC-125) transcripts encoding many of the predicted transporters increased after 24 h of P deprivation. Significant increases in *PTB2*, *PTB3*, *PTB4*, and *PTB5* mRNAs were observed for wild-type cells after 24 h of P deprivation, with little increase or a declining abundance in the *psr1-1* mutant subjected to the same conditions. These results demonstrate that PSR1 is involved in controlling the abundance of these transcripts and that this control is probably exerted at the level of transcription (since PSR1 is a MYB domain-containing transcription factor). Interestingly, *PTB2-PTB3* and *PTB5-PTB4* are contiguous, with the transcript from the proximal gene of each pair (*PTB2* and *PTB5*) being most strongly elevated after 24 h of P starvation. No significant increase in the level of *PTB1* mRNA was observed during P stress, which is in agreement with the report of Kobayashi et al. (24), and the *PTB6* transcript could not be detected (data not shown).

In contrast, expression patterns of the *PTA* transcripts varied considerably during P stress (Table 2). In wild-type cells, *PTA1* transcript abundance was reduced 1,000-fold during P deprivation but only 2- to 6-fold in the *psr1* mutant (depending on whether the 24-h time point is compared to the wild-type or *psr1-1* 0-h control), suggesting that PSR1 may play a role in the repression of this gene. *PTA2* and *PTA3* mRNA levels declined slightly or remained unchanged after P deprivation, whereas *PTA4* expression increased significantly in both the wild-type and *psr1* mutant strains. Interestingly, the level of the *PTA4* transcript was 10- to 20-fold higher in P-starved wild-type cells

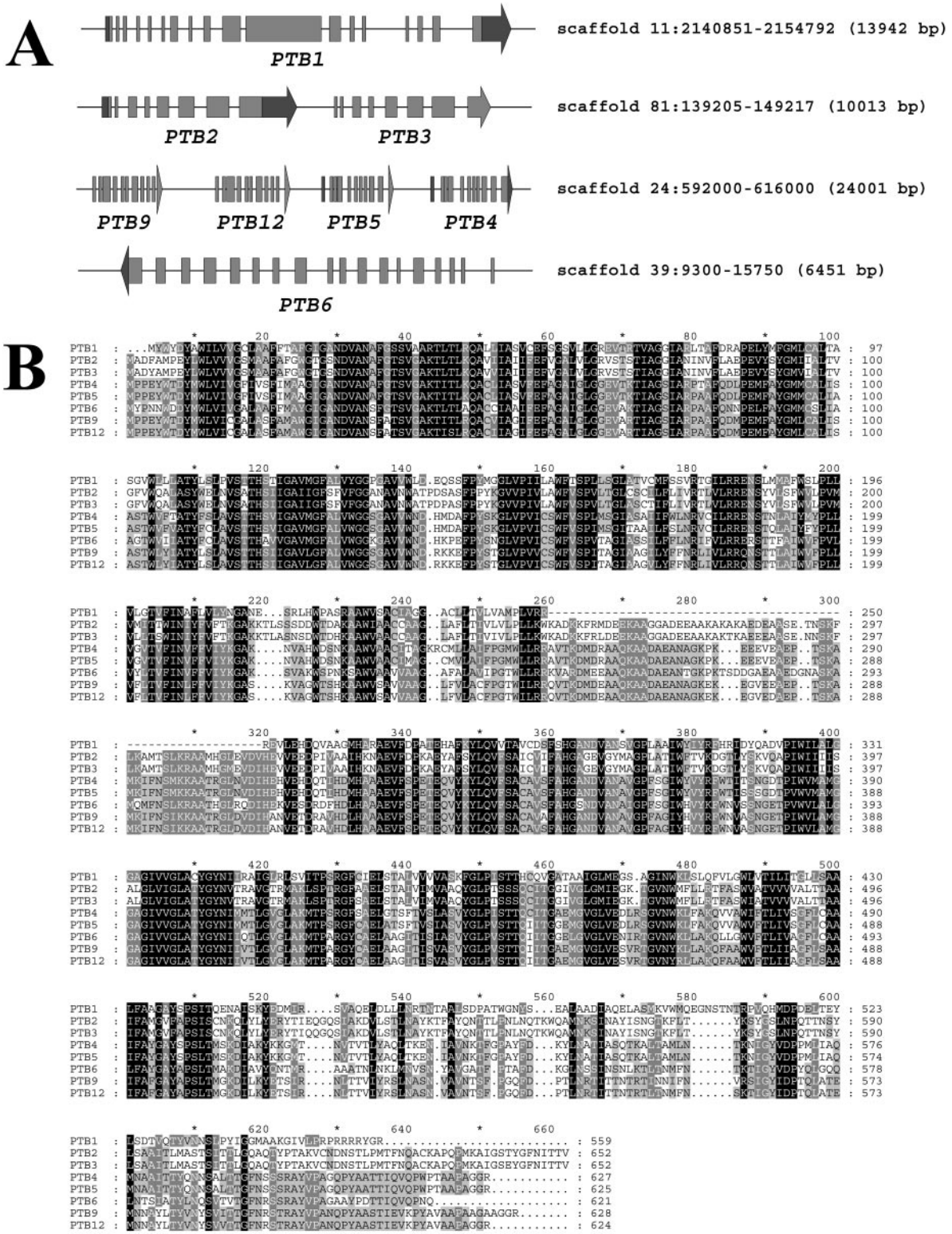

FIG. 3. P_i transporter type B paralogs. (A) Schematic representation of the arrangement of *PTB* genes in the *C. reinhardtii* genome. The direction of transcription is indicated by the direction of the arrows. Coding sequences are represented by light gray boxes or arrows, the connecting lines correspond to introns, and dark gray boxes or arrows correspond to the 5′ and 3′ untranslated regions of each gene. The gene models for *PTB1* and *PTB2* are based on BLASTN alignments with the cDNA sequences (accession no. AB074880 and AB074881, respectively); the other gene models were assembled using a combination of GreenGenie gene structure prediction, TBLASTN alignments with PTB1 and PTB2, and alignments of EST sequences. (B) CLUSTALW alignment of eight PTB proteins. A 1,107-amino-acid sequence between residues 252 and 1,358 which is not similar to any of the other PTB sequences was removed from the PTB1 sequence prior to construction of the alignment (represented by dashes). Black shading denotes 100% sequence identity or conservative replacement in all sequences, dark gray shading with white letters denotes sequence conservation in at least six of eight sequences, and light gray shading with black letters denotes sequence conservation in at least four of eight sequences.

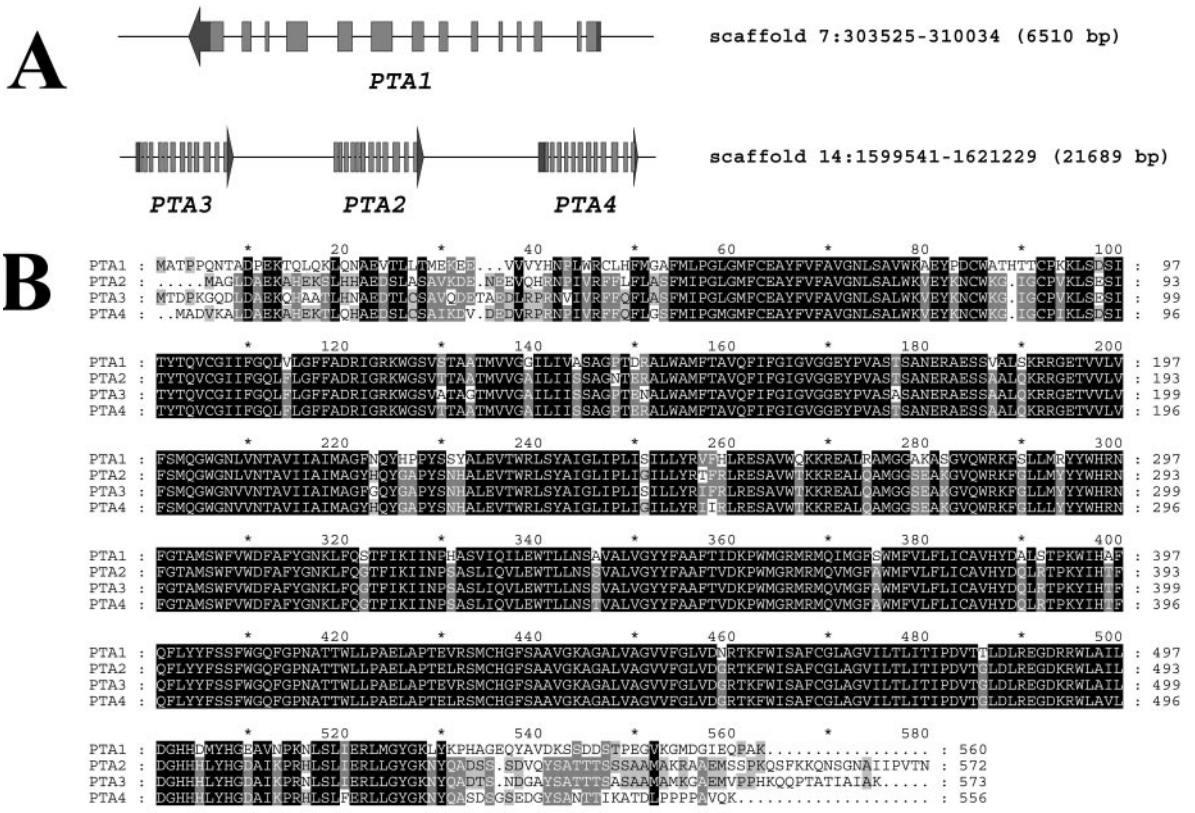

FIG. 4. P_i transporter type A paralogs. (A) Schematic representing the arrangement of *PTA* genes in the *C. reinhardtii* genome. The *PTA1*, *PTA2*, and *PTA3* gene models are based on alignments with the cDNA sequences (accession no. AB074874, AB074875, and AB074876, respectively); the *PTA4* model was constructed based on similarity to the other *PTA* genes and to matching EST sequences. (B) CLUSTALW alignment of four PTA proteins, as described in the legend to Fig. 3.

than in P-starved *psr1* cells. It is possible that PSR1 is partially responsible for the induction of this gene, or alternatively, the *psr1* mutant may be unable to fully activate the expression of *PTA4* due to secondary stress responses that occur in the mutant following the imposition of P deprivation. In sum, the results suggest that the PTA transporters (except, perhaps, for PTA4) are likely to not contribute significantly to the high-affinity P_i transport activity observed soon after the imposition of P deprivation. These transporters could be involved in transport under nutrient-replete conditions or may modulate P_i transport between specific cellular compartments. Alternatively, it is possible that some of the PTA proteins transport solutes other than P_i.

The qPCR analysis demonstrated that *PHOX* transcript levels markedly increase by 24 h of P depletion (Table 2). This increase is under the control of PSR1, and the extent of the increase may reflect the very low basal level of the transcript present in P-replete cells. To confirm that the *C. reinhardtii PHOX* gene encodes the major inducible alkaline phosphatase activity, immunoblot analysis was performed on whole-cell extracts from P_i-replete versus P-starved wild-type and *psr1-1* mutant strains with antiserum raised to a *V. carteri* PHOX peptide (Fig. 5) (18). The immunoblot revealed a polypeptide of ~190 kDa that cross-reacts with anti-PHOX antibodies; this polypeptide was observed in extracts of wild-type cells starved for P (but not in extracts of cells grown on complete medium), and the band was not detected for the *psr1-1* strain under any

TABLE 2. Putative P_i scavenging-related transcript abundance after 24 h of P_i deprivation

Gene	Fold change in transcript abundance					
	CC-125[a]		*psr1-1* mutant (compared to CC-125 at 0 h)[b]		*psr1-1* mutant (compared to *psr1-1* mutant at 0 h)[c]	
	Expt 1	Expt 2	Expt 1	Expt 2	Expt 1	Expt 2
PHOX	4420	5793	0.39	1.41	2.30	5.08
PTB1	1.00	1.60	0.59	1.72	1.62	1.80
PTB2	46.9	52.3	1.11	1.49	0.68	0.80
PTB3	6.96	11.6	ND[d]	ND[d]	ND[d]	ND[d]
PTB4	14.7	15.5	0.28	0.37	0.73	1.04
PTB5	292	832	1.19	2.83	3.96	4.14
PTA1	0.0007	0.0012	0.16	0.19	0.55	0.80
PTA2	1.23	1.68	0.32	0.68	0.54	0.83
PTA3	0.48	0.53	0.36	0.48	0.62	0.97
PTA4	27.0	46.9	2.07	4.76	3.72	9.51
PSR1	3.48	42.2	0.07	0.60	NA[e]	NA[e]

[a] Expression of transcripts from CC-125 grown for 24 h with P_i deprivation relative to CC-125 control RNA at 0 h, as determined by quantitative real-time PCR. Relative expression levels were calculated by the $2^{-\Delta\Delta C_T}$ method.

[b] Relative expression of transcripts from *psr1-1* mutant grown for 24 h without P_i compared to CC-125 control RNA at 0 h.

[c] Relative expression of transcripts from *psr1-1* mutant grown for 24 h without P_i compared to *psr1-1* mutant RNA at 0 h.

[d] The *PTB3* PCR product was not detected (ND) in the *psr1-1* mutant. A misprimed PCR product was sequenced and determined to be derived from *PTB2* (data not shown).

[e] NA, not applicable, since the *PSR1* transcript was not detected in the *psr1-1* RNA sample at 0 h.

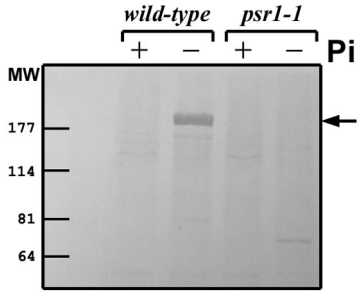

FIG. 5. Immunodetection of PHOX. The immunoblot was created by using anti-PHOX antiserum (18) and whole-cell extracts from either P-replete (+) or P-deprived (24 h) (−) wild-type and *psr1* mutant cells.

conditions tested. The cross-reacting band was not detected on a control blot without the anti-*PHOX* antibody (data not shown), excluding the possibility that residual alkaline phosphatase activity remained in the *C. reinhardtii* protein extract after the proteins were transferred to the membrane (since an alkaline phosphatase color reaction was used to detect the secondary antibody). Together, these data strongly suggest that *C. reinhardtii PHOX* encodes the major inducible alkaline phosphatase activity of *C. reinhardtii*.

Expression of genes encoding potential "electron valves." The *psr1* mutants were originally isolated based on their inability to either perform high-affinity P_i uptake or synthesize extracellular phosphatase activity following exposure of *C. reinhardtii* to P starvation conditions (46, 54). The *psr1-1* and *psr1-2* (two different alleles) mutants were able to down-regulate photosynthetic electron transport and did not show apparent signs of photodamage or reduced viability relative to wild-type cells, even after 10 days of growth without P. This is in contrast to the phenotype of the *sac1* strain, which is unable to acclimate to sulfur deprivation; this mutant is very sensitive to light conditions, and in the absence of sulfate, it dies under moderate light intensities (50 to 100 μmol photons m^{-2} s^{-1}) (10). As a consequence, PSR1 was originally considered to regulate specific and not general P deprivation responses. However, as noted above, microarray analyses revealed that a number of transcripts encoding proteins associated with conditions of hyperstimulation of photosynthetic electron transport increased and that these increases appeared to be under PSR1 control. qPCR was used to establish a more quantitative assessment of the levels of these transcripts during P deprivation (Table 3). The *AOX1* transcript increased three- to fivefold in wild-type cells starved for P for 24 h relative to unstarved cells. P deprivation had little effect on the level of this transcript in the *psr1-1* strain, corroborating the results of the microarray experiments (Table 1). In contrast, the *AOX2* transcript was not detected under any cell growth conditions used (data not shown). The transcripts from both genes encoding the plastid terminal oxidases (PTOX1 and PTOX2) (25, 38) were detected by qPCR, but in contrast to the microarray results, where a 13-fold upregulation of *PTOX1* mRNA was observed in wild-type cells after 48 h of P starvation (Table 1), *PTOX1* transcripts appeared to increase only 2.5- to 3-fold, while the level of the *PTOX2* transcript was not consistently higher in wild-type cells starved for P than in unstarved cells. A small change in *PTOX2* transcript levels was also observed in the *psr1-1* mutant. The discrepancies between the microarray and qPCR results may be a consequence of the fact that the qPCR is much more sensitive than microarray analyses. For example, the fluorescence signal of *PTOX1* in the microarray experiments was comparable to the background at most time points. Consequently, even small changes in the abundance of the transcript registered as large changes in the observed ratios. *HYD1* and *HYD2* represent another pair of paralogous genes that appeared to be differentially expressed during P deprivation. Consistent with the microarray results, qPCR measurements showed that the *HYD1* mRNA did not change over the course of P deprivation in wild-type cells. In contrast, *HYD2* mRNA abundance increased 8- to 13-fold in P-starved wild-type cells. These observations support the inference drawn from the microarray results that PSR1 may directly or indirectly influence the expression of the *HYD2* gene. The abundance of both *HYD1* and *HYD2* declined severely (~5- to 10-fold) in the *psr1-1* strain, possibly reflecting some contribution of PSR1 to the maintenance of basal levels of *HYD* expression. PSR1-dependent regulation was also observed for two genes encoding the starch phosphorylase homologs GPLV1 and GPLV2. Based on both microarray and qPCR data, the *GPLV1* transcript was elevated four- to ninefold in wild-type cells after 24 h of P deprivation but remained approximately constant in the *psr1-1* mutant during P deprivation. Similarly, the *GPLV2* transcript increased threefold in wild-type cells and remained constant in the *psr1-1* strain during P deprivation. Therefore, in most of the cases that we have examined, where transcript abundance for one member of a gene family is potentially regulated by PSR1, the regulation of the other is independent of PSR1.

Three genes encoding glyceraldehyde-3-phosphate dehydro-

TABLE 3. "Electron valve"-encoding transcript abundance after 24 h of P_i deprivation

Gene	Fold change in transcript abundance					
	CC-125[a]		*psr1-1* mutant (compared to CC-125 at 0 h)[b]		*psr1-1* mutant (compared to *psr1-1* mutant at 0 h)[c]	
	Expt 1	Expt 2	Expt 1	Expt 2	Expt 1	Expt 2
AOX1	3.00	5.28	0.75	1.46	1.14	1.41
PTOX1	2.55	3.22[d]	0.19	2.23	0.14	1.48
PTOX2	1.22	3.35	0.08	0.69	2.21	3.31
GAP1	36.6	72.0	0.21	0.21	0.17	0.71
GAP2	4.14	5.90	0.27	0.41	0.36	0.64
GAP3	1.38	1.80	0.31	0.53	0.39	0.99
HYD1	1.19	1.57	0.11	0.16	0.08	0.15
HYD2	8.31	13.5	0.09	0.14	0.10	0.18
GPLV1	4.07	8.88	1.38	1.80	1.60	2.46
GPLV2	3.25	3.32	0.59	1.17	0.87	1.08
DHAR	4.77	6.50	1.57	3.03	3.11	3.73

[a] Expression of transcripts from CC-125 grown for 24 h without P_i relative to CC-125 control RNA at 0 h, as determined by quantitative real-time PCR. Relative expression levels were calculated by the $2^{-\Delta\Delta C_T}$ method.

[b] Relative expression of transcripts from the *psr1-1* mutant grown for 24 h without P_i compared to CC-125 control RNA at 0 h.

[c] Relative expression of transcripts from the *psr1-1* mutant grown for 24 h without P_i compared to *psr1-1* mutant RNA at 0 h.

[d] *PTOX1* transcripts were from CC-125 and the *psr1-1* mutant grown for 48 h without P_i relative to CC-125 or *psr1-1* mutant RNA at 0 h.

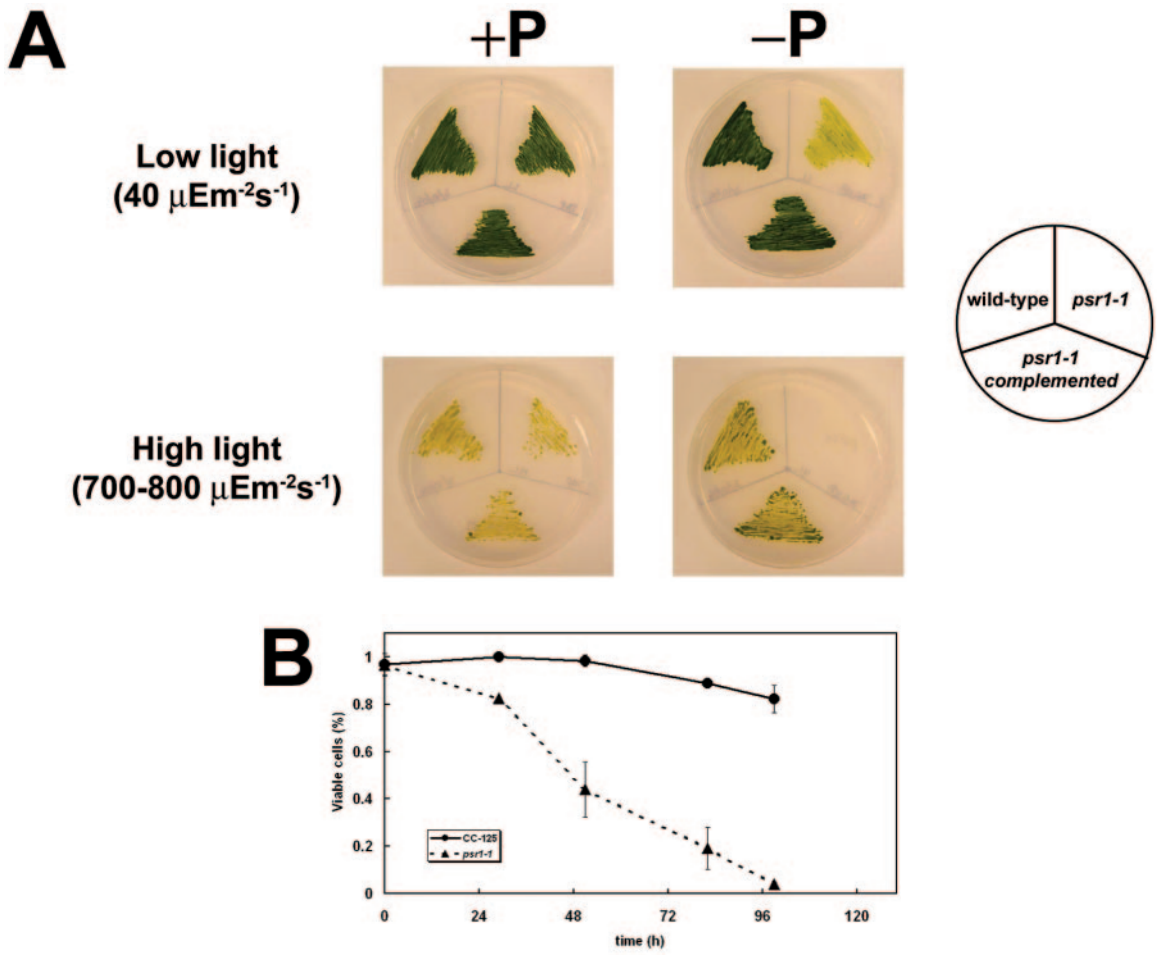

FIG. 6. Light sensitivity of *psr1* during P deprivation. (A) Comparison of growth of wild-type cells, *psr1* mutant cells, and a *psr1*-complemented strain on solid TAP medium (left panels) or TA medium supplemented with 10 μM glucose-1-phosphate (right panels). Plates were grown for 6 days under the indicated light intensities. (B) Graph showing viability of wild-type (solid line, circles) and *psr1-1* (dashed line, triangles) cells during growth in TA (P-free) medium at a constant light intensity of ~700 μmol photons m^{-2} s^{-1}.

genases (GAPs) have been identified in the *C. reinhardtii* genome. The GAP1 and GAP3 polypeptides have N-terminal extensions. *GAP3* has been characterized biochemically and encodes a subunit of the chloroplastic NADP-dependent GAP that functions in the Calvin-Benson cycle (27). Although GAP1 is predicted to be targeted to the mitochondrion, the prediction has a low confidence score (TargetP score, 0.635), and generally for *C. reinhardtii*, prediction programs are not reliable in discriminating between mitochondrial and chloroplast targeting (12). *GAP2* has no presequence and is likely to encode the cytosolic form of the enzyme that functions in glycolysis. *GAP1* is the only member of this gene family that is represented on the microarray, and the level of its transcript appeared to increase five- to sixfold during P starvation in wild-type cells, but not in the *psr1-1* mutant (Table 1). Based on qPCR, the *GAP1* mRNA increased 37- to 72-fold in wild-type cells after 24 h of P deprivation. The qPCR data suggest that the *GAP2* mRNA increases approximately four- to sixfold in wild-type cells, but not in *psr1-1* mutant cells. In contrast, the *GAP3* RNA abundance is relatively constant in both wild-type cells and the *psr1-1* mutant (Table 3). These results suggest that *GAP1* and *GAP2*, but not *GAP3*, are under the control of PSR1 and also raise the possibility that PSR1 influences the expression of glycolytic enzymes. Interestingly, although some plants express a nonphosphorylating GAPN enzyme to "bypass" the NAD^+- and P_i-dependent enzyme in glycolysis (11, 17) and although a GAPN gene homolog is present in the *C. reinhardtii* genome, the mRNA from this gene declined 5- to 10-fold during P deprivation, independent of PSR1 (data not shown). These results suggest that *C. reinhardtii* uses mechanisms to regulate carbon flux through the glycolytic pathway that are different from those described for vascular plants.

Sensitivity of *psr1-1* mutant to high light intensity. The discovery that the mRNAs of a variety of genes with a putative electron valve function increased during P deprivation in a PSR1-dependent manner raised questions concerning the role that PSR1 might play in controlling general responses to P deficiency. Therefore, we compared the sensitivities of the *psr1-1* mutant, wild-type cells, and a *PSR1*-complemented strain to elevated light intensities during P deprivation (Fig. 6). In moderate light (40 μmol photons m^{-2} s^{-1}) on TA medium supplemented with a limiting amount of a hydrolyzable P_i

TABLE 4. TargetP prediction of subcellular targeting of potential P_i transporters

Protein	TargetP score[a]				Prediction[b]
	Chloroplast	Mitochondrion	Secretory pathway	Other	
PTA1	0.112	0.069	0.022	0.933	Any other location (RC 1)
PTA2	0.000	0.549	0.711	0.179	Secreted (RC 5)
PTA3	0.061	0.086	0.041	0.935	Any other location (RC 1)
PTA4	0.069	0.047	0.070	0.910	Any other location (RC 1)
PTB1	0.008	0.019	0.953	0.060	Secreted (RC 1)
PTB2	0.004	0.008	0.913	0.395	Secreted (RC 3)
PTB3	0.012	0.035	0.808	0.361	Secreted (RC 3)
PTB4	0.009	0.009	0.970	0.317	Secreted (RC 2)
PTB5	0.002	0.013	0.982	0.280	Secreted (RC 2)
PTB6	0.001	0.016	0.980	0.346	Secreted (RC 2)

[a] TargetP scores were determined as described previously (12).
[b] TargetP prediction, with reliability class (RC) indicated, from 1 to 5, where 1 indicates the strongest prediction.

source (10 μM glucose-1-phosphate), the *psr1-1* mutant survived but grew more slowly than wild-type cells or the complemented strain and also arrested at a lower cell density. In contrast, when the three strains were exposed to high light intensities (700 to 800 μmol photons m^{-2} s^{-1}) for 3 days during P deprivation, the *psr1-1* mutant became bleached and died, while little loss of viability occurred for wild-type cells and the complemented mutant (Fig. 6A). Viability staining of cultures grown in liquid TA medium under high light intensities confirmed that 80 to 90% of *psr1-1* cells died by day 6 of P depletion, whereas 80% of the wild-type cells and the complemented cells survived these conditions (Fig. 6B).

DISCUSSION

We have used genomic information to help elucidate the effects of P_i starvation on gene expression in *C. reinhardtii*. Microarray studies were used to identify genes that are either positively or negatively regulated as cells become starved for P and to define those genes that appear to be controlled by the transcription factor PSR1 (46, 54). Similar microarray analyses of P deficiency responses have been performed with *Arabidopsis thaliana* (19, 52). A few qualitative similarities are observed between the responses in *C. reinhardtii* and those in plants, including induction of genes encoding P-scavenging enzymes and down-regulation of photosynthetic genes and genes involved in cytoplasmic and chloroplast translation, along with modulation of some genes involved in carbon metabolism (52). Overall, the overlap between P deficiency-responsive target genes in *C. reinhardtii* and those in plants appears to be limited, perhaps reflecting differences in P storage and distribution between the multicellular plants and the unicellular algae. It should also be considered that all of the array experiments in question were performed with subgenome arrays and that some common target genes may not have been represented on the plant or *C. reinhardtii* arrays.

In initial studies of *psr1* mutants, no increased sensitivity to moderate light intensities was observed, and accordingly, PSR1 was not considered to play a role in protecting cells against photodamage. However, the microarray data demonstrated that a class of genes encoding potential "electron valves" appeared to be activated during P starvation in a PSR1-dependent manner. These genes encode enzymes that assist in the dissipation of potentially harmful species that may accumulate as a consequence of photosynthetic and respiratory electron transfer reactions under conditions that might restrict the use of products generated by these reactions. Microarray analyses identified transcripts from 210 genes that exhibited differential accumulation during P deprivation of threefold or greater in the wild-type and *psr1-1* strains (Fig. 1). This represents approximately two-thirds the number of transcripts that exhibited a threefold change during sulfur starvation (56), although some transcripts are common between the two sets of data. The commonality may reflect responses to general intracellular stress conditions that may be generated by both types of nutrient deprivation.

P_i-scavenging genes. A total of 10 potential P_i transporters were identified in the *C. reinhardtii* genome (Fig. 3 and 4); at least six are differentially expressed during P deprivation. The transcripts for four of the *PTB* and one of the *PTA* genes increased in abundance in P-starved cells. Increased levels of these transcripts appeared to require PSR1. It is not clear which of these transporters (or groups of transporters) contributes most significantly to the high-affinity P_i uptake observed in P-deprived cells. In *S. cerevisiae*, which grows best in low-pH environments, the major secreted phosphatase, PHO5, has an acidic pH optimum, and the dominant high-affinity transporter is the Pho84 H^+/P_i symporter (PTA type) (3, 6). The *S. cerevisiae* Pho89 Na^+/P_i cotransporter (PTB type) may play a less significant role in P_i uptake, as it operates best in alkaline conditions (29). However, the situation may be very different for *C. reinhardtii*, which thrives in neutral or basic environments and secretes a predominant alkaline phosphatase during P deprivation (39). This may, in part, explain the bias towards activation of the *PTB* genes in *C. reinhardtii*; like Pho89, the PTB enzymes would be expected to display superior P_i uptake at an alkaline pH. Currently, there is no definitive evidence regarding the cellular location of the PTB and PTA proteins, but TargetP v1.01 predicts with high confidence that all of the PTB proteins are routed along the secretory pathway (Table 4), making these strong candidates for components of a plasma membrane (or vacuolar membrane)-associated P_i starvation-inducible P_i uptake system. Based on both microarray and qPCR analyses, *PTB2* and *PTB5* transcripts increase in abundance >20- and several hundredfold, respectively, following exposure of cells to P deprivation conditions (Tables 1 and

2). No change in P_i uptake characteristics was observed with a *ptb1* mutant of *C. reinhardtii* (15), implying that the gene product is not essential for the elevated P_i uptake observed when cells begin to experience P limitations. Congruent with this result, the *PTB1* transcript level does not respond significantly to P deprivation conditions. Kobayashi et al. (24) have suggested that PTB1 may be involved in intracellular P_i transport. The paired genomic clusters of the *PTB2*/*PTB3* and *PTB4*/*PTB5* genes, the high sequence identity between the members of the pairs, and the presence of numerous, scattered *PTB* gene fragments in close proximity suggest that this gene family has undergone a recent expansion. The different patterns of transcript abundance in response to P limitation defined for the individual members of this gene family suggest that the encoded proteins may play divergent roles in P_i uptake and distribution within the cell.

The family of transporters designated PTA (Pho84 homologs) for *C. reinhardtii* has been designated Pht for *A. thaliana*. These proteins in *A. thaliana* have been implicated in both high- and low-affinity P_i transport, and the genes encoding these proteins are specifically expressed in plant roots (47). For *C. reinhardtii*, only PTA2 is predicted to be routed through the secretory pathway, and this prediction has a low confidence score (Table 4). Furthermore, changes in transcript levels during P deprivation were varied for the different *PTA* genes. There was a strong PSR1-dependent decline in *PTA1* mRNA and no significant change in the level of the *PTA2* transcript. Microarray experiments suggested a PSR1-dependent increase in *PTA3* mRNA levels, but this observation was not confirmed by qPCR measurements (Tables 1 and 2). In cases where the qPCR and microarray data do not corroborate each other, we generally find that the fluorescence signal of the corresponding gene on the microarray is low (comparable to the background), and this can result in faulty ratios. The *PTA4* transcript increased significantly in both wild-type and *psr1-1* mutant cells exposed to P deprivation, although the increase was consistently higher for wild-type cells. We have previously demonstrated that the activation of high-affinity P_i uptake in P-deficient cells requires PSR1 (46). Therefore, in general, the patterns of *PTA* transcript accumulation in wild-type and mutant cells (except, perhaps, for PTA4) and the predicted subcellular locations of the PTA polypeptides are not consistent with a role for these transporters in P starvation-inducible P_i uptake. It is more likely that the *PTA* gene products contribute to either low-affinity P_i uptake or intracellular trafficking of P_i. For example, *PTA1* might encode a component of a low-affinity P_i uptake system that is expressed under nutrient-replete conditions and repressed when the cells are starved for P. A more detailed biochemical approach needs to be initiated in order to develop a precise understanding of the functions of the different PTA and PTB transport proteins.

The *C. reinhardtii PHOX* gene encodes a homolog of the PHOX protein of *V. carteri*, and the level of mRNA encoding this protein increases dramatically during P deprivation (Table 2). Immunological analyses using *V. carteri* PHOX antibodies suggest that this protein represents the previously characterized secreted, Ca^{2+}-dependent alkaline phosphatase of *C. reinhardtii* (39).

C. reinhardtii also maintains internal stores of polyphosphate in cytosolic organelles, akin to the polyphosphate bodies of fungi and the acidocalciosomes found in trypanosomatids and apicomplexan parasites (43). Although nothing is known about the synthesis and regulation of polyphosphate in *C. reinhardtii*, it is interesting that the mRNA encoding VCX1, a potential vacuolar H^+/Ca^{2+} antiporter (Table 1), also increased during P deprivation. In yeast, this protein is responsible for controlling cytosolic Ca^{2+} levels in the presence of high extracellular concentrations of Ca^{2+} (30). This finding raises the possibility that the VCX1 protein serves to maintain vacuolar sequestration of the Ca^{2+} that is released from polyphosphate bodies in the vacuole as P_i is enzymatically generated during P deprivation-triggered polyphosphate degradation.

Stress-related gene expression. A number of transcripts encoding stress-related proteins increased during P starvation in both the wild-type strain and the *psr1-1* mutant; the levels of these transcripts do not appear to be under PSR1 control. These transcripts include those encoding two putative 22-kDa chloroplast-localized heat shock proteins, a glutathione *S*-transferase, an E3 ubiquitin ligase, and two protease homologs (Table 1, proteolysis/stress-related proteins). Chaperones and proteases may be required to sequester and eliminate misfolded or damaged proteins (9, 13). While most of these transcripts only significantly increased at the final time point following elimination of P from the growth medium (48 h) in the wild-type strain, they became elevated by 12 h of P deprivation in the *psr1-1* mutant. These results suggest that while both strains show a generalized stress response, the mutant senses more extreme stress conditions at earlier times after the elimination of P from the medium; this more rapid response may reflect the inability of the mutant to scavenge P_i from both intracellular and extracellular resources.

A number of physiological responses have been shown to be elicited by P starvation. With respect to photosynthetic activity, there is a depletion of PS II reaction centers, accumulation of Q_B nonreducing centers, increased nonphotochemical quenching, and transition of the energy transfer characteristics of the antenna chlorophyll from state I to state II. These characteristics are indicators of excess excitation of the photosynthetic apparatus and suggest that the photosynthetic electron transport chain is hyperreduced, even under conditions of moderate light intensity (53). Gene expression analysis supports this idea, since, in addition to the P starvation-responsive chaperones and proteases, we observed increases in some transcripts that were also elevated at high light intensities (21). For example, there was an increase in transcripts encoding the granule-bound starch synthase I (STA2), which may help to relieve excess excitation by stimulating starch synthesis, and LHCSR2, a protein related to light-harvesting complex (LHC) antenna proteins that may have a photoprotective function (Table 1) (21, 41). The transcripts for these proteins are also elevated during sulfur deprivation (56). Although the kinetics of increase in STA2 mRNA were similar for wild-type cells and the *psr1-1* mutant, the increase in transcript abundance was observed earlier in *psr1-1* mutant cells than in wild-type cells (12 h versus 24 h). Furthermore, the increased transcript levels were sustained in the mutant cells, even up to 48 h; at 48 h, the mRNA level in wild-type cells dropped to below the 2.5-fold threshold (Table 1). These results again suggest that the signal transduction pathway that regulates some of the deprivation-induced genes becomes active more rapidly and that the re-

sponse is sustained longer following the initiation of P starvation of *psr1-1* than that of wild-type cells.

Electron valves and radical-scavenging enzymes. In addition to potential stress-related transcripts that increase in both wild-type cells and *psr1-1* mutant cells, another set of transcripts encoding proteins implicated in photoprotection is elevated exclusively in wild-type cells during P deprivation. These photoprotective proteins may act as "electron valves" that serve to drain electrons from the photosynthetic and mitochondrial electron transfer chains, decreasing the potential dangers associated with hyperreduction of electron carriers and the generation of triplet chlorophyll molecules. An enhanced capacity for alternative respiration in iron-starved *C. reinhardtii* has been reported previously (51), and mutants of tobacco plants with a defective alternative oxidase were unable to sustain normal respiratory rates upon P deprivation (37). We observed increased transcript levels from the alternative oxidase gene *AOX1* in wild-type cells starved for P for 24 h. In contrast, the *psr1-1* mutant exhibited a transient increase in *AOX1* mRNA after 4 h of P deprivation, but this increase was not maintained. Increased alternative oxidase activity during P starvation may perform a number of functions, including preventing the accumulation of reactive oxygen species in the mitochondria, allowing continued flux of metabolites through the tricarboxylic acid cycle for generating organic carbon "backbones," and controlling carotenoid biosynthesis and the rate of ATP formation under conditions in which the availability of P_i may be limiting (7, 23, 25). Increased levels of the *AOX1* transcript were previously reported during S starvation (56), and upon transfer of cells from growth on ammonium to growth on nitrate (1). Surprisingly, *AOX1* is the only transcript encoding a known mitochondrial protein that was significantly upregulated in these experiments, suggesting that the control of mitochondrial processes during P deprivation may be regulated largely by posttranscriptional mechanisms.

Increased levels of transcripts encoding PTOX1, a putative plastid terminal oxidase, were also observed in wild-type P-starved cells, but not in the *psr1-1* mutant. The PTOX1 protein may represent the terminal oxidase activity responsible for chlororespiration (8, 38). This terminal oxidase may relieve redox pressure associated with photosynthetic electron transfer by withdrawing electrons from plastoquinol and combining them with O_2. PTOX1 is a homolog of a plastid terminal oxidase in plants, encoded by the *IMMUTANS* gene, which is also implicated in carotenoid synthesis (23), raising the possibility that PTOX1 induction during P starvation in *C. reinhardtii* might play a role in the production of photoprotective carotenoids.

A third potential electron valve that may increase during P deprivation in cells with active PSR1 is the Fe hydrogenase, encoded by *HYD2* (*HYDB*). The *C. reinhardtii* hydrogenases catalyze the transfer of electrons from PS I to water to produce H_2 gas under anaerobic/microaerobic conditions, and they are believed to help reoxidize the plastoquinol pool when the cytoplasm of the cell is highly reducing, especially during anaerobic or hypoxic growth (14, 16, 20). The hydrogenase activity might increase plastoquinol oxidation during P starvation, relieving the block on linear electron transfer and helping to prevent the production of reactive oxygen species. The activation of *HYD2* gene expression might be a by-product of the production of a microaerobic environment within cells as oxygen evolution declines during P deprivation and respiration consumes oxygen faster than it is being produced. However, were this the case, it would be expected that *HYD1* expression would be induced as well, but this was not observed in either microarray or qPCR experiments. *HYD2* mRNA abundance is much greater in wild-type cells than in the *psr1-1* mutant (compare transcript levels in Tables 1 and 3), suggesting that PSR1 plays a role in maintaining expression of this gene (or the conditions required for its expression).

As discussed above, *C. reinhardtii* shows increased *STA2* mRNA expression during P deprivation; the STA2 protein is involved in the synthesis of starch. Elevating starch synthesis can help control the accumulation of excess reductant in the cell and limit the production of reactive oxygen species. However, P starvation of wild-type cells also leads to elevated mRNA for both *GPLV*, encoding a starch phosphorylase, and an alpha amylase gene. Both of these gene products are involved in the conversion of starch to sugar. Therefore, the starved cells may also have an increased capacity to actively degrade storage starch, which could be important for maintaining the flux through the starch synthesis pathway. Finally, the transcript for dehydroascorbate reductase also increases in P-starved wild-type cells but not in the *psr1-1* mutant. This enzyme is involved in recycling of ascorbate, an antioxidant that plays an important role in scavenging reactive oxygen species in the chloroplast. Together, the results presented above demonstrate that increases in mRNAs for proteins that have an electron valve function and that help the cells manage an elevated redox state appear to be normal aspects of the P starvation responses of *C. reinhardtii*. Although a causative relationship between the activation of these pathways and resistance to high light intensities remains to be established, it is intriguing that conditions of high light intensity are lethal to the *psr1* mutant and that the transcripts from many of these genes do not significantly increase in the *psr1-1* mutant.

Photosynthesis. A number of genes represented on the array encoding proteins with photosynthetic functions appear to be differentially expressed during P starvation. While down-regulation of PS II function and abundance has been demonstrated previously (53), we did not observe changes in mRNA levels for nuclear genes encoding structural subunits of PS II during P starvation. Instead, transcripts from several *LHCA* genes, encoding components of the LHC of PS I (LHC I), and *PSAE* and *PSAK* genes, encoding subunits of PS I, declined in both P-starved wild-type cells and *psr1-1* mutant cells. A reduced level of the *CHL27* (*CRD1*) transcript was also observed. *CHL27* encodes a component of the chlorophyll biosynthetic enzyme Mg-protoporphyrin IX monomethylester cyclase (49) and has been reported to play a role in controlling the interaction between the PS I reaction center and LHC I. Therefore, reduced levels of CHL27 protein would be expected to result in a weaker energetic connection between the LHC I antennae and core PS I (32). The transcripts for proteins that are minor subunits of the cytochrome b_6f complex, i.e., PETO and PETN, also appear to decline in wild-type cells, with the *PETM* and *PETC* transcripts showing similar trends (although the level of the *PETM* and *PETC* mRNAs only declined by 50% over the time course [see Table S1 in the supplemental material]). Indeed, transcripts encoding all PSB, PSA, and PET

proteins represented by elements on the array declined in both wild-type cells and the *psr1-1* strain.

Aberrant gene expression in the *psr1-1* mutant. Twenty-nine transcripts exhibited increased accumulation in *psr1-1* but not wild-type cells during P starvation (Fig. 1). The increased levels of these transcripts may be a consequence of the more extreme stress conditions experienced by the *psr1-1* mutant than by wild-type cells since the mutant would not be able to properly acclimate as P levels in the medium declined. The aberrant metabolic status of the mutant strain may also trigger specific signaling pathways in addition to more general stress response pathways. Increased levels of transcripts encoding phytoene synthase, a key regulatory enzyme in carotenoid biosynthesis, and homogentisic acid geranylgeranyl transferase, an enzyme required for tocopherol biosynthesis, may reflect the cell's response to elevated reducing conditions and a greater tendency to form reactive oxygen molecules, both of which are associated with nutrient deprivation conditions (34). Interestingly, the *psr1-1* mutant also exhibited increased mRNAs for a subset of genes associated with sulfur acquisition and assimilation (Table 1, sulfur metabolism). This finding may reflect a change in the energy status of the cell and the inability of the mutant to efficiently take up and activate SO_4^{2-}. However, since we observed an increase in transcript levels for only a subset of the genes associated with sulfur-deficient conditions, it is possible that there is a more specific link between the P and S deprivation pathways. Understanding these links may help us to decipher the networks of interactions among stress responses and the hierarchy of responses observed.

ACKNOWLEDGMENTS

J.L.M. was supported by a Life Sciences Research Foundation fellowship from the U.S. Department of Energy, and this work was supported by U.S. Department of Agriculture grant 2002-35301-12178 and National Science Foundation grant MCB 0235878, both awarded to A.R.G.

We thank Chung-Soon Im, Wirulda Pootakham, Steve Pollock, Nakako Shibagaki, and Jeff Shrager for technical assistance and helpful comments on the manuscript and Armin Hallmann and Sabeeha Merchant for the kind gift of antibodies. We also thank the Joint Genome Institute for providing access to a prerelease of version 3 of the *Chlamydomonas* draft genome sequence.

REFERENCES

1. **Baurain, D., M. Dinant, N. Coosemans, and R. F. Matagne.** 2003. Regulation of the alternative oxidase *Aox1* gene in *Chlamydomonas reinhardtii*. Role of the nitrogen source on the expression of a reporter gene under the control of the *Aox1* promoter. Plant Physiol. **131:**1418–1430.
2. **Benjamini, Y., and Y. Hochberg.** 1995. Controlling the false discovery rate: a practical and powerful approach to multiple testing. J. R. Stat. Soc. Ser. B **57:**289–300.
3. **Berhe, A., U. Fristedt, and B. L. Persson.** 1995. Expression and purification of the high-affinity phosphate transporter of *Saccharomyces cerevisiae*. Eur. J. Biochem. **227:**566–572.
4. **Bieleski, R. L.** 1973. Phosphate pools, phosphate transport, and phosphorus availability. Annu. Rev. Plant Physiol. Plant Mol. Biol. **24:**225–252.
5. **Brooks, A..** 1996. Effects of phosphorus nutrition on ribulose-1,5-bisphosphate carboxylase activation, photosynthetic quantum yield and amounts of some Calvin cycle metabolites in spinach leaves. Aust. J. Plant Physiol. **13:**221–237.
6. **Bun-ya, M., M. Nishimura, S. Harashima, and Y. Oshima.** 1991. The *PHO84* gene of *Saccharomyces cerevisiae* encodes an inorganic phosphate transporter. Mol. Cell, Biol. **11:**3229–3238.
7. **Carol, P., and M. Kuntz.** 2001. A plastid terminal oxidase comes to light: implications for carotenoid biosynthesis and chlororespiration. Trends Plant Sci. **6:**31–36.
8. **Cournac, L., G. Latouche, Z. Cerovic, K. Redding, J. Ravenel, and G. Peltier.** 2002. In vivo interactions between photosynthesis, mitorespiration, and chlororespiration in *Chlamydomonas reinhardtii*. Plant Physiol. **129:**1921–1928.
9. **Craig, E. A., H. C. Eisenman, and H. A. Hundley.** 2003. Ribosome-tethered molecular chaperones: the first line of defense against protein misfolding? Curr. Opin. Microbiol. **6:**157–162.
10. **Davies, J. P., F. H. Yildiz, and A. Grossman.** 1996. Sac1, a putative regulator that is critical for survival of *Chlamydomonas reinhardtii* during sulfur deprivation. EMBO J. **15:**2150–2159.
11. **Duff, S. M. G., G. B. G. Moorhead, D. D. Lefebvre, and W. C. Plaxton.** 1989. Phosphate starvation inducible "bypasses" of adenylate and phosphate dependent glycolytic enzymes in *Brassica nigra* suspension cells. Plant Physiol. **90:**1275–1278.
12. **Emanuelsson, O., H. Nielsen, S. Brunak, and G. von Heijne.** 2000. Predicting subcellular localization of proteins based on their N-terminal amino acid sequence. J. Mol. Biol. **300:**1005–1016.
13. **Fink, A. L.** 1999. Chaperone-mediated protein folding. Physiol. Rev. **79:**425–449.
14. **Forestier, M., P. King, L. Zhang, M. Posewitz, S. Schwarzer, T. Happe, M. L. Ghirardi, and M. Seibert.** 2003. Expression of two [Fe]-hydrogenases in *Chlamydomonas reinhardtii* under anaerobic conditions. Eur. J. Biochem. **270:**2750–2758.
15. **Fujiwara, S., I. Kobayashi, S. Hoshino, T. Kaise, K. Shimogawara, H. Usuda, and M. Tsuzuki.** 2000. Isolation and characterization of arsenate-sensitive and resistant mutants of *Chlamydomonas reinhardtii*. Plant Cell Physiol. **41:**77–83.
16. **Ghirardi, M. L., L. Zhang, J. W. Lee, T. Flynn, M. Seibert, E. Greenbaum, and A. Melis.** 2000. Microalgae: a green source of renewable H_2. Trends Biotechnol. **18:**506–511.
17. **Habenicht, A., U. Hellman, and R. Cerff.** 1994. Non-phosphorylating GAPDH of higher plants is a member of the aldehyde dehydrogenase superfamily with no sequence homology to phosphorylating GAPDH. J. Mol. Biol. **237:**165–171.
18. **Hallmann, A.** 1999. Enzymes in the extracellular matrix of Volvox: an inducible, calcium-dependent phosphatase with a modular composition. J. Biol. Chem. **274:**1691–1697.
19. **Hammond, J. P., M. J. Bennett, H. C. Bowen, M. R. Broadley, D. C. Eastwood, S. T. May, C. Rahn, R. Swarup, K. E. Woolaway, and P. J. White.** 2003. Changes in gene expression in Arabidopsis shoots during phosphate starvation and the potential for developing smart plants. Plant Physiol. **132:**578–596.
20. **Happe, T., and A. Kaminski.** 2002. Differential regulation of the Fe-hydrogenase during anaerobic adaptation in the green alga *Chlamydomonas reinhardtii*. Eur. J. Biochem. **269:**1022–1032.
21. **Im, C. S., Z. Zhang, J. Shrager, C. W. Chang, and A. R. Grossman.** 2003. Analysis of light and CO_2 regulation in *Chlamydomonas reinhardtii* using genome-wide approaches. Photosyn. Res. **75:**111–125.
22. **Jacob, J., and D. W. Lawlor.** 1993. In vivo photosynthetic electron transport does not limit photosynthetic capacity in phosphate-deficient sunflower and maize leaves. Plant Cell Environ. **16:**785–795.
23. **Josse, E. M., A. J. Simkin, J. Gaffe, A. M. Laboure, M. Kuntz, and P. Carol.** 2000. A plastid terminal oxidase associated with carotenoid desaturation during chromoplast differentiation. Plant Physiol. **123:**1427–1436.
24. **Kobayashi, I., S. Fujiwara, K. Shimogawara, T. Kaise, H. Usuda, and M. Tsuzuki.** 2003. Insertional mutagenesis in a homologue of a Pi transporter gene confers arsenate resistance on Chlamydomonas. Plant Cell Physiol. **44:**597–606.
25. **Kuntz, M.** 2004. Plastid terminal oxidase and its biological significance. Planta **218:**896–899.
26. **Lenburg, M. E., and E. K. O'Shea.** 1996. Signaling phosphate starvation. Trends Biochem. Sci. **21:**383–387.
27. **Li, A. D., and L. E. Anderson.** 1997. Expression and characterization of pea chloroplastic glyceraldehyde-3-phosphate dehydrogenase composed of only the B-subunit. Plant Physiol. **115:**1201–1209.
28. **Livak, K. J., and T. D. Schmittgen.** 2001. Analysis of relative gene expression data using real-time quantitative PCR and the $2^{-\Delta\Delta C_T}$ method. Methods **25:**402–408.
29. **Martinez, P., and B. L. Persson.** 1998. Identification, cloning and characterization of a derepressible Na^+-coupled phosphate transporter in *Saccharomyces cerevisiae*. Mol. Gen. Genet. **258:**628–638.
30. **Miseta, A., R. Kellermayer, D. P. Aiello, L. Fu, and D. M. Bedwell.** 1999. The vacuolar Ca^{2+}/H^+ exchanger Vcx1p/Hum1p tightly controls cytosolic Ca^{2+} levels in *S. cerevisiae*. FEBS Lett. **451:**132–136.
31. **Miura, K., A. Rus, A. Sharkhuu, S. Yokoi, A. S. Karthikeyan, K. G. Raghothama, D. Baek, Y. D. Koo, J. B. Jin, R. A. Bressan, D.-J. Yun, and P. M. Hasegawa.** 2005. The *Arabidopsis* SUMO E3 ligase SIZ1 controls phosphate deficiency responses. Proc. Natl. Acad. Sci. USA **102:**7760–7765.
32. **Moseley, J. L., T. Allinger, S. Herzog, P. Hoerth, E. Wehinger, S. Merchant, and M. Hippler.** 2002. Adaptation to Fe-deficiency requires remodeling of the photosynthetic apparatus. EMBO J. **21:**6709–6720.
33. **Nicholas, K. B., H. B. Nicholas, Jr., and D. W. Deerfield II.** 1997. GeneDoc: analysis and visualization of genetic variation. EMBNEW.NEWS **4:**14.
34. **Niyogi, K. K.** 1999. Photoprotection revisited: genetic and molecular approaches. Annu. Rev. Plant Physiol. Plant Mol. Biol. **50:**333–359.
35. **Ogawa, N., J. DeRisi, and P. O. Brown.** 2000. New components of a system

for phosphate accumulation and polyphosphate metabolism in *Saccharomyces cerevisiae* revealed by genomic expression analysis. Mol. Biol. Cell **11:** 4309–4321.
36. **Oshima, Y.** 1997. The phosphatase system in *Saccharomyces cerevisiae*. Genes Genet. Syst. **72:**323–334.
37. **Parsons, H. L., J. Y. Yip, and G. C. Vanlerberghe.** 1999. Increased respiratory restriction during phosphate-limited growth in transgenic tobacco cells lacking alternative oxidase. Plant Physiol. **121:**1309–1320.
38. **Peltier, G., and L. Cournac.** 2002. Chlororespiration. Annu. Rev. Plant Biol. **53:**523–550.
39. **Quisel, J. D., D. D. Wykoff, and A. R. Grossman.** 1996. Biochemical characterization of the extracellular phosphatases produced by phosphorus-deprived *Chlamydomonas reinhardtii*. Plant Physiol. **111:**839–848.
40. **Raghothama, K. G.** 1999. Phosphate acquisition. Annu. Rev. Plant Physiol. Plant Mol. Biol. **50:**665–693.
41. **Richard, C., H. Ouellet, and M. Guertin.** 2000. Characterization of the LI818 polypeptide from the green unicellular alga *Chlamydomonas reinhardtii*. Plant Mol. Biol. **42:**303–316.
42. **Rubio, V., F. Linhares, R. Solano, A. C. Martin, J. Iglesias, A. Leyva, and J. Paz-Ares.** 2001. A conserved MYB transcription factor involved in phosphate starvation signaling both in vascular plants and in unicellular algae. Genes Dev. **15:**2122–2133.
43. **Ruiz, F. A., N. Marchesini, M. Seufferheld, Govindjee, and R. Docampo.** 2001. The polyphosphate bodies of *Chlamydomonas reinhardtii* possess a proton-pumping pyrophosphatase and are similar to acidocalcisomes. J. Biol. Chem. **276:**46196–46203.
44. **Sambrook, J., E. F. Fritsch, and T. Maniatis.** 1989. Molecular cloning: a laboratory manual. Cold Spring Harbor Laboratory Press, Cold Spring Harbor, N.Y.
45. **Schachtman, D. P., R. J. Reid, and S. M. Ayling.** 1998. Phosphorus uptake by plants: from soil to cell. Plant Physiol. **116:**447–453.
46. **Shimogawara, K., D. D. Wykoff, H. Usuda, and A. R. Grossman.** 1999. *Chlamydomonas reinhardtii* mutants abnormal in their responses to phosphorus deprivation. Plant Physiol. **120:**685–694.
47. **Shin, H., H. S. Shin, G. R. Dewbre, and M. J. Harrison.** 2004. Phosphate transport in Arabidopsis: Pht1;1 and Pht1;4 play a major role in phosphate acquisition from both low- and high-phosphate environments. Plant J. **39:** 629–642.
48. **Thompson, J. D., D. G. Higgins, and T. J. Gibson.** 1994. CLUSTAL W: improving the sensitivity of progressive multiple sequence alignment through sequence weighting, position-specific gap penalties and weight matrix choice. Nucleic Acids Res. **22:**4673–4680.
49. **Tottey, S., M. A. Block, M. Allen, T. Westergren, C. Albrieux, H. V. Scheller, S. Merchant, and P. E. Jensen.** 2003. Arabidopsis CHL27, located in both envelope and thylakoid membranes, is required for the synthesis of protochlorophyllide. Proc. Natl. Acad. Sci. USA **100:**16119–16124.
50. **Vogel, K., and A. Hinnen.** 1990. The yeast phosphatase system. Mol. Microbiol. **4:**2013–2018.
51. **Weger, H. G., and G. S. Espie.** 2000. Ferric reduction by iron-limited Chlamydomonas cells interacts with both photosynthesis and respiration. Planta **210:**775–781.
52. **Wu, P., L. Ma, X. Hou, M. Wang, Y. Wu, F. Liu, and X. W. Deng.** 2003. Phosphate starvation triggers distinct alterations of genome expression in Arabidopsis roots and leaves. Plant Physiol. **132:**1260–1271.
53. **Wykoff, D. D., J. P. Davies, A. Melis, and A. R. Grossman.** 1998. The regulation of photosynthetic electron transport during nutrient deprivation in *Chlamydomonas reinhardtii*. Plant Physiol. **117:**129–139.
54. **Wykoff, D. D., A. R. Grossman, D. P. Weeks, H. Usuda, and K. Shimogawara.** 1999. Psr1, a nuclear localized protein that regulates phosphorus metabolism in Chlamydomonas. Proc. Natl. Acad. Sci. USA **96:**15336–15341.
55. **Zer, H., and I. Ohad.** 2003. Light, redox state, thylakoid-protein phosphorylation and signaling gene expression. Trends Biochem. Sci. **28:**467–470.
56. **Zhang, Z., J. Shrager, M. Jain, C. W. Chang, O. Vallon, and A. R. Grossman.** 2004. Insights into the survival of *Chlamydomonas reinhardtii* during sulfur starvation based on microarray analysis of gene expression. Eukaryot. Cell **3:**1331–1348.